NASA Technical Paper 1970

AVRADCOM Technical Report 81-A-2

April 1982

A Study of Resonant-Cavity and Fiberglass-Filled Parallel Baffles as Duct Silencers

Paul T. Soderman

NASA

NASA Technical Paper 1970

AVRADCOM Technical Report 81-A-2

1982

A Study of Resonant-Cavity and Fiberglass-Filled Parallel Baffles as Duct Silencers

Paul T. Soderman
Ames Research Center

Aeromechanics Laboratory
AVRADCOM Research and Technology Laboratories
Moffett Field, California

National Aeronautics and Space Administration

Scientific and Technical Information Branch

TABLE OF CONTENTS

SYMBOLS

A	silencer attenuation, dB
a	perforated plate hole diameter, m
c	sound speed, m/sec
D	cavity depth, m
d	liner depth or half baffle thickness, m
f	frequency, Hz
h	half-duct width between baffles, m
IL	silencer insertion loss, dB
k	ω/c wave number, m^{-1}
Lp	sound pressure level, dB, $Re\ 2 \times 10^{-5}$ N/m^2
ℓ	length of acoustic lining, m
m	horizontal duct mode number
NR	silencer noise reduction, dB
n	vertical duct mode or cavity mode number
P	perforated plate porosity, percent $\times$ 100
q_o	dynamic pressure upstream of silencer corrected to area equal to test-section area, N/m^2
R	acoustic resistance, mks rayls (NS/m^3)
Re	Reynolds number
R_1	flow resistivity, mks rayls/m
St	Strouhal number
t	perforated plate thickness, m
U	average flow speed between baffles, m/sec
U_o	flow speed upstream of silencer corrected to duct area equal to test-section area, m/sec
V	cavity volume, m^3
X	acoustic reactance, mks rayls
y	duct height, m
Z	acoustic impedance, mks rayls
z	$2h$, duct width between baffles, m
γ	acoustic propagation constant, m^{-1}
Δ dB	change in sound level, dB
ΔP	total or static pressure drop through silencer, N/m^2
δ	end correction for perforated plate hole depth, m
λ	acoustic wavelength, m
μ	dynamic viscosity of air, NS/m^2
ρc	characteristic impedance of air, 407 mks rayls

A STUDY OF RESONANT-CAVITY AND FIBERGLASS-FILLED PARALLEL BAFFLES AS DUCT SILENCERS

Paul T. Soderman*

Ames Research Center
and
Aeromechanics Laboratory
AVRADCOM Research and Technology Laboratories

Acoustical performance and pressure drop were measured for two types of splitters designed to attenuate sound propagating in ducts – resonant-cavity baffles and fiberglass-filled baffles. Arrays of four baffles were evaluated in the 7- by 10-Foot Wind Tunnel Number 1 at Ames Research Center at flow speeds from 0 to 41 m/sec. The baffles were 2.1 m high, 305 to 406 mm thick, and 3.1 to 4.4 m long. Emphasis was on measurements of silencer insertion loss as affected by variations of such parameters as baffle length, baffle thickness, perforated skin geometry, cavity size and shape, cavity damping, wind speed, and acoustic field directivity. An analytical method for predicting silencer performance is described and compared with measurements.

Unlike small, single-orifice resonators, the undamped, resonant-cavity baffles attenuated sound over a broad frequency range. With the addition of cavity damping in the form of 25-mm foam linings, the insertion loss above 250 Hz of the resonant-cavity baffles was improved 2 to 7 dB compared with the undamped baffles; the loss became equal to or greater than the insertion loss of comparable size fiberglass baffles at frequencies above 250 Hz. Variations of cavity size and shape showed that a series of cavities with triangular cross-sections (i.e., variable depth) were superior to cavities with rectangular cross sections (i.e., constant depth). In wind, the undamped, resonant-cavity baffles generated loud cavity-resonance tones; the tones could be eliminated by cavity damping. Duct-resonance tones were also generated by configurations that had solid skin over portions of the baffle surfaces. The effects of skin porosity, baffle length, and baffle thickness are documented.

A series of five wind-tunnel tests has been conducted at Ames Research Center for the purpose of developing inlet and exhaust silencers for the 80- by 120-Foot Wind Tunnel being built at Ames. The new wind tunnel, described by Mort et al. in reference 1, will have a 110 by 41 m inlet and a 52 by 41 m exhaust, which must be muffled by duct splitters to reduce the exposure of the community to drive-fan and powered-model noise. Soderman and Page described the expected drive-fan noise in reference 2. The acoustical requirements for the silencers were established by Scharton et al. (ref. 3).

Because of the immense size of the facility, it was decided that a study should be made of the numerous parameters affecting duct splitters so that the silencers would provide the proper acoustic and aerodynamic performance at least cost. Early in the program, it was recognized that alternatives to the conventional baffle filled with fibrous material should be investigated to avoid, if possible, the problems of erosion and clogging of bulk absorbers described by Mechel in reference 4. T. Scharton, then under contract to Ames, developed the idea of using duct splitters composed of resonant cavities covered by perforated-plate skins that dissipate acoustic energy.

In reference 5, Scharton and Sneddon describe several basic analytical and experimental studies they made of the concept. Using that work as a guide, this author planned a series of detailed, large-scale experiments on resonant-cavity and fiberglass-filled baffles. It was impractical to construct a very large array of duct splitters to simulate the inlet or exhaust silencers

*Presently with the National Aeronautics and Space Administration, Ames Research Center.

for the 80- by 120-Foot Wind Tunnel. Instead, a set of four baffles, with full-scale length, thickness, and spacing, was evaluated in the Ames 7- by 10-Foot Wind Tunnel Number 1. This report describes the results of the wind-tunnel tests along with the analytical methods used to guide the experiments. Implications of these results for silencer design are described in reference 6. It should be noted that the silencer geometries evaluated were constrained to be mechanically simple and durable and to block no more than 44% of the simulated inlet duct or to block no more than 33% of the simulated exhaust duct. These last constraints were based on estimates of acceptable pressure loss for the 80- by 120-Foot Wind Tunnel. The acoustical design goal was an insertion loss spectrum that would attenuate 80- by 120-Foot Wind Tunnel drive-fan noise by 16 dBA. The results described here are also applicable to other duct systems and other design goals because an effort was made to document the change in silencer attenuation due to changes in baffle geometry, baffle composition, flow speed, and acoustic source directivity. One of the resonant-cavity configurations was described by Soderman and Scharton in reference 7, but performance was not documented. That documentation is included here.

MODELS AND APPARATUS

Fiberglass-Filled Baffle Geometry

Figures 1(a) and 1(b) are photographs of the fiberglass-filled baffles in the wind-tunnel test section. The baffles – 3 m long, 305 mm thick – were placed on 914 mm centers, as shown in figure 1(c). The passages between the baffles were 610 mm wide. The fiberglass filler had a density of 25.6 kg/m^3 and a flow resistivity of 10^4 mks rayls/m. The fiberglass was installed as 76-mm-thick blankets stacked together. Because of a center septum, the fiberglass depth was 152 mm, viewed from each flow passage. The wall baffles were actually half baffles because the cavity behind the center septum was sealed off from the test section. Baffles of this geometry would block 33% of the full-scale inlet or exhaust. Because of the constraint of the 7- by 10-Foot Wind Tunnel test section size, the baffles actually blocked 40% of the duct. Except for the solid skin on the nose, each baffle had 1.2-mm-thick perforated-steel skin with an open area of 33%; the open area was composed of 2.4-mm-diameter holes on 4.0-mm staggered centers (see fig. 1(c) for the meaning of "staggered" centers). The effect of 0.03-mm-thick plastic (Mylar) sheet between the fiberglass and perforated skin was also evaluated.

Resonant-Cavity Baffle Geometry

The resonant-cavity baffles were varied in size and composition. Figures 2(a)-2(c) show the configurations tested and the letter codes used to identify them. The geometric parameters were as follows.

Length– The baffle lengths ranged from 3.0 to 4.3 m. However, because the noses and tails of most configurations were nonporous, the acoustically active sections varied from 1.8 to 3.0 m.

Thickness and spacing– Configurations A–K were 305 mm thick on 914-mm centers, as were the fiberglass baffles. Each passage between the baffles was 610 mm wide. An array of baffles would block 33% of a large duct, but, as mentioned above, the true blockage of the test section was 40%. Configurations L–P were designed to simulate 406-mm-thick baffles on 914-mm centers having 508-mm flow passages and 44% duct blockage. However, this was impossible to achieve in the 3.0-m-wide test section. Therefore, the thickness of the two center baffles was kept at 406 mm and the three flow passages were kept at 508 mm by reducing the thickness of the two wall baffles to 356 mm, as shown in figure 3. The resulting duct blockage was 50%. The implications of this compromise are discussed in the section on accuracy.

Cavity shape– As seen in figures 2(a)-2(c), the cavities had triangular, rectangular, or trapezoidal cross sections. In all cases, the volumes were continuous from floor to ceiling. The orientation of the cavity partitions were alternated from baffle to baffle, as shown in figure 3.

Perforated skin– To achieve the proper lining impedance, low-porosity perforated-steel sheets were used to cover the cavities. Two porosities were evaluated – open areas of 2.6% and 4.9%. Most of the data were acquired with perforations that were 1.6 mm in diameter; a few acoustic measurements were made with perforate hole diameters of 3.2 mm. The perforated skin thickness ranged from 0.6 mm to 1.2 mm. All these dimensions are noted in figures 2(a)-2(c).

Sound absorptive liners– Blankets of foam or fiberglass were attached to the diagonal septa forming the back wall of the cavities in order to assess the importance of cavity damping. In some cases, the liners were attached to the end wall of the cavities.

Acoustic Source

In the foreground of figure 1(b) is the sound source used to determine silencer insertion loss. Four loudspeakers were installed in an aerodynamically shaped enclosure that was 190 mm thick, 890 mm high, and 1.11 m long. The two low-frequency speakers (one on each side) or two high-frequency speakers (one on each side) were driven simultaneously with uncorrelated, random (pink) noise filtered in octave or third-octave bands. With the enclosure streamwise, the sound reflected off the test-section walls creating a semireverberant sound field. Some data were taken, wind off, with the enclosure rotated 90°, which tended to cause the sound to beam along the duct axis. The actual directivity of the source was not measured. The source was positioned upstream or downstream of the baffles to simulate an exhaust or inlet sound field.

Instrumentation

Four microphones upstream and four microphones downstream were used to measure the noise reduction of the silencer, as shown in figures 1(a) and 1(b) (photographs) and in figure 4(a) (schematic). The microphones shown inside the center passage were used initially to measure the distribution of sound through the silencer. They were removed early in the program and replaced by a traversing microphone for selected runs. The 12.7-mm-diameter omnidirectional microphones had aerodynamic nose cones pointed upstream. The microphone signals were monitored, recorded, and processed as shown in figure 4(b).

EXPERIMENTAL METHOD

Acoustic Data Reduction

The test-section background noise, at each wind speed, was measured with the silencer in place. The microphone sound levels were then corrected for background noise in the normal manner (see ref. 8), unless the background noise was within 3 dB of the total noise (source and wind on), in which case the data were rejected. The average noise level at each duct cross section was determined by first finding the average of the pressure-squared signals from the four microphones, and then computing the decibel level of the average. It was possible to measure the insertion loss of the silencer by measuring the sound in the duct with and without the silencer installed between the source and microphones. Since frequent removal of the baffles was inconvenient, and because the source output could change over a period of days or weeks, the insertion loss was computed in the following manner. First, the difference in noise level across the silencer (noise reduction) was measured and then corrected for sound attenuation due to distance between the two sets of microphones, the sound attenuation having been measured in the wind tunnel with the silencer removed. That correction was 2 dB for the inlet simulation and 1 to 3 dB for the exhaust simulation. Next, the data were corrected for reverberation buildup measured on the source side of the baffles; approximately 1 dB above 200 Hz. The final value is the muffler insertion loss. To summarize:

$$IL = NR - \Delta dB_1 - \Delta dB_2 \qquad (1)$$

where

ΔdB_1 = sound attenuation due to distance between microphone arrays, silencer out

ΔdB_2 = reverberation buildup due to silencer

Accuracy

Four factors affected the accuracy of the insertion loss data: (1) microphone and other instrumentation errors; (2) sound variation with time and microphone position; (3) background noise; and (4) flanking noise (e.g., sound that propagated around the wind-tunnel circuit, bypassing the baffles). To minimize these effects, the following steps were taken for each factor.

Factor (1): The instrumentation system was calibrated at least twice a day to maintain a ±0.5 dB accuracy. The condenser-microphone heads were frequently dried in a desiccant chamber to stabilize their response.

Factor (2): The data were averaged for 8 sec with a real-time frequency analyzer, which resulted in third-octave band levels with a negligible variation with time. The spatial variation of noise at each duct cross section depended on the diffusion of the reverberant sound. Below 200 Hz, the variation from microphone to microphone was as much as 8 dB. Above 200 Hz, the variation dropped to 3 dB. By averaging the pressure-squared signal from four microphones before computing the average sound level, the standard deviation of the sound levels relative to that average below 200 Hz was typically 2 to 3 dB; above 200 Hz it was typically 1 to 2 dB. When the source was rotated so the sound beamed along the duct axis, the standard deviation of sound level increased 1 or 2 dB because the sound field was less diffuse.

Factor (3): The background noise was only a problem at the downstream microphones at high speeds because of wake impingement. If the background noise was within 3 dB of the total noise, the microphone data were rejected. If the background noise was less than that, the data were corrected as necessary.

Factor (4): The flanking noise was insignificant, as was determined by blocking off the silencer with a high-transmission-loss barrier and measuring the level of sound that one way or another bypassed the silencer.

A more difficult question is: How well did the experiment simulate the performance of an array of baffles in a large duct? For our purpose, the baffles were full-scale in length, thickness, and spacing. However, the simulation was imperfect with respect to (1) the nature of the sound source, (2) the duct blockage, and (3) the relatively short height of the baffles. Without full-scale data, the exact accuracy of the simulation is unknown. However, with respect to these three limitations, the following is noted.

Limitation (1): With the acoustic source enclosure streamwise, the sound reflected off the test-section walls, striking the baffles from many angles, which is similar to placing a muffler in a large, semireverberant duct. With the enclosure rotated 90°, the sound tended to beam along the duct axis. Thus, there are two sets of data in this report representing extreme situations. The bulk of the data was taken with a semireverberant sound field because that was closest to the wind-tunnel problem being addressed.

Limitation (2): As mentioned in a previous section, the duct blockage of the baffles was different from the blockage of an infinite array of baffles – 40% instead of 33% for the 305-mm baffles and 50% instead of 44% for the 406-mm-thick baffles. Consider the 305-mm-thick baffles. The proper duct blockage would have required five baffles in a 3.7-m-wide test section, with the fifth baffle recessed in the wall, instead of four baffles in a 3.0-m-wide test section (see fig. 1(c)). However, each flow passage would be identical to those used in these studies, and the attenuation of each passage would not change, except for the effects due to incidence of the entering sound waves; that is, walls 3.7 m apart would reflect the sound into the baffles with slightly different angles than walls 3.0 m apart. Hence, the insertion loss measured in the actual and ideal ducts should be very similar. Similar arguments hold for the 406-mm-thick baffles.

Limitation (3): Because of the 2.1-m height of the baffles, the test-section floor and ceiling reflected sound waves, which, in a much larger duct, would have been free to pass unhindered except for the baffles themselves. Fortunately, the steel floor and ceiling had very low sound absorption. Moreover, since the distance from the floor to ceiling was comparable to the baffle length, only a very small number of sound waves made more than a few floor and ceiling reflections while traversing the silencer. Except for nearly vertical propagation, the reflected sound rays in the model silencer negotiated a distance past the baffles, and with similar energy decay, that was the same as it would be in a full-scale silencer.

RESULTS AND DISCUSSION

This section describes an analytical method for predicting the acoustic impedance and attenuation of fiberglass silencers and resonant-cavity silencers and presents experimental results of the parametric studies of baffle sets in the 7- by 10-Foot Wind Tunnel.

Analytical Prediction of Silencer Performance

Fiberglass-filled silencer– The size, spacing, and composition of the fiberglass-filled baffles, shown in figure 1(c), were very similar to a design recommended for the 80- by 120-Foot Wind Tunnel by Scharton et al. (ref. 3). The duct blockage of 33% is usually less than desirable for a duct silencer, but was necessary because of the importance to

wind-tunnel operation of high flow speed. The baffle geometry and fiberglass flow resistance were based on an analytical optimization procedure described by Schultz (ref. 9) and on data documented by Doelling and Bolt (ref. 10). There are various sources of data and empirical methods, such as references 10 and 11, available for the prediction of fiberglass-baffle performance. However, the further one deviates from the configurations used to acquire the data, the less accurate are the empirical methods. Therefore, a search was made for an analytical method with a minimum of empiricism so that silencer performance could be predicted for a wide range of parameters and configurations. The one adopted was the Kurze method described in references 9 and 12. Kurze gives a closed-form solution for the attenuation of a duct lined on two opposite sides as follows:[1]

$$A = 8.69\,\ell\,Re(\gamma) \tag{2}$$

where

A = silencer attenuation, dB

ℓ = duct length

$Re(\gamma)$ = real part of the propagation constant γ

and

$$\gamma = jk\left\{1 - \left(\frac{2}{kh}\right)^2 \left[1 + \frac{1}{1 + (4Z/jkh\rho c)} \pm \left(1 + \frac{1}{[1 + (4Z/jkh\rho c)]^2}\right)^{1/2}\right]\right\}^{1/2} \tag{3}$$

where

j = $\sqrt{-1}$, complex number

k = ω/c, wave number

h = half duct width between linings

ρc = characteristic impedance of air, 407 mks rayls

[1] In reference 9, the equation is slightly different because the silencer attenuation D is actually attenuation per length of duct equal to length h.

and

$$Z = R + jX, \text{ linear impedance} \tag{4}$$

The proper sign in equation (3) is the one that gives the smaller value of $Re(\gamma)$. The resistance term R in equation (4) can be described by the weak resistance of the holes in the perforated skin R_h plus the stronger resistance of the fiberglass liner R_ℓ:

$$R = R_h + R_\ell \tag{5}$$

For low (linear) sound levels and low flow speeds, Ingard and Ising (ref. 13) give the following expression for R_h:

$$R_h = \frac{(8\mu\rho\omega)^{1/2}[1 + (t/a)]}{P} \tag{6}$$

where

μ = dynamic viscosity of the gas

t = plate thickness

a = hole diameter

P = perforation porosity

For a full depth bulk liner, Shultz (ref. 9) gives the following value of R_ℓ:

$$R_\ell = \frac{R_1 d}{3} \tag{7}$$

where

R_1 = flow resistivity of liner

d = liner depth (assumed equal to half baffle thickness)

The resistance of the 0.152-m-deep fiberglass filler used in the experiment is 507 mks rayls, according to equation (7). The reactance term X, in equation (4), can be separated into a term describing the stiffness of the air layer in the liner X_ℓ and a term describing the mass reactance of the air in the perforated plate holes X_p.

$$X = X_\ell + X_p \tag{8}$$

Following Shultz (ref. 9):

$$X_{\ell} = -0.8\,\rho c \cot(kd) \tag{9}$$

and from reference 13:

$$X_p = \frac{\omega\rho(t+\delta)}{P} \tag{10}$$

where $\delta = 0.85\,a$ (no flow); $\delta = 0.40\,a$ (with flow).

The solution of equation (2), using the above impedance model, is plotted in figure 5 along with the measured insertion loss of the fiberglass-filled silencer. It was assumed that the 3.0-m-long baffles, which included 300-mm solid noses and 900-mm tapered tails, were equivalent to a 2.1-m-long lining, 152 mm deep (half baffle thickness), on opposite walls of a duct with a 610-mm-wide flow passage. Also included in figure 5 is an empirical correction curve from Doelling (ref. 14), which represents typical *transverse* mode decay as measured in a wide range of mufflers. The correction is meant to be added to plane-wave attenuation estimates. Kurze's method (ref. 12) applies only to the plane-wave propagation and underpredicts the mid- and high-frequency attenuation because of the transverse acoustic modes generated by the streamwise loudspeaker enclosure. Doelling's estimate is closer in that frequency range, but falls below the data. However, with the source rotated 90° and beaming at the silencer, the measured attenuation at frequencies above 1 kHz dropped 3 dB below Doelling's estimate. This illustrates the difficulty of predicting silencer performance in a world in which silencer performance depends strongly on the nature of the sound field entering the silencer. Under the circumstances, Doelling's scheme is a good compromise at midfrequencies to high frequencies because the predicted attenuation fell midway between the measured attenuation for the two types of sound fields – semireverberant and semiplaner. At lower frequencies, the Kurze method is more applicable because of the preponderance of acoustical plane waves. However, that method predicted a peak attenuation 4 dB higher and a peak frequency slightly higher than measured. All in all, the combination of the two prediction schemes gives fair agreement with the experimental results.

Resonant-cavity silencer– The analytical method used to estimate bulk-absorber performance was also employed to guide the experimental studies of resonant-cavity baffles because, for the configurations envisioned, there were no data or empirical methods available. Moreover, the resonant-cavity silencer is, for the most part, a dissipative silencer like the fiberglass silencer. Equations (2) through (4) were used with impedance terms appropriate for a duct lining composed of variable-depth, empty cavities covered by a perforated plate. At low flow speeds, the resistance of the lining is due entirely to the resistance of the air in the perforated plate holes, which is given by equation (6). However, as the flow speed rises, the resistance of the orifices increases due to the interaction between oscillating acoustic waves in the orifices and the grazing flow. The interaction is illustrated in the photographs of Baumeister and Rice (ref. 15). Scharton and Sneddon (ref. 5) derived the following expression for perforated plate resistance based on the work of Rogers and Hersh (ref. 16):

$$R = \frac{0.67\,\rho U}{P} \tag{11}$$

where U = average flow speed between baffles.

Rice (ref. 17) derived a similar expression with the factor 0.5 instead of 0.67 in equation (11). The proper value of resistance for a given set of conditions is the larger of the two values given by equations (6) and (11). The resistance of the fiberglass filler shown in figure 1(c) was estimated to be 507 mks rayls. To get the same resistance from a perforated plate at a flow speed of 17 m/sec requires a porosity of 2.7% (according to eq. (11)). That was the starting point for the experimental study described in the following sections.

The reactance terms used for the resonant-cavity silencer were the same as those used for the fiberglass silencer, except for the stiffness term (equation (9)), which was modified to:

$$X_{\ell} = -\rho c \cot(kd) \tag{12}$$

The analytical method of Kurze (ref. 12) was applied to a 3.1-m-long duct lining (two walls) spaced 610 mm apart and composed of five equal

length cavities on each side, with variable depth corresponding to baffle configuration D. Figure 6(a) shows the computed attenuation for two different perforated plate porosities: 3% and 5%. The plate with the 5% open area gave much better attenuation because the resistance of the perforations, 272 mks rayls, was closer to the theoretically optimum value of 167 mks rayls at 250 Hz given by Cremer's equation (ref. 9):

$$Z = R + jX = \rho c\,(0.92 - j\,0.77)\,\frac{2h}{\gamma} \qquad (13)$$

where Z is the theoretically optimum duct lining impedance for maximum attenuation.

The reactance of both linings in figure 6(a) were similar. The insertion loss[2] differences between the two linings determined experimentally were not as great as indicated by figure 6(a), as will be shown in a later section. The effect of wind speed on predicted attenuation is shown in figure 6(b). Also plotted is Doelling's curve (ref. 14) for transverse-mode attenuation. A comparison with the measured insertion loss for configuration D in figure 6(c) indicates that the analytical results did not agree with the data, especially at the peak frequency. Furthermore, the data were much less sensitive to wind speed than predicted. Despite this lack of agreement, the analytical methods did show that a skin of very low porosity was needed on the baffles to get adequate acoustic resistance. However, it was apparent that the primary effort for studying the resonant-cavity baffles would have to be experimental rather than analytical.

Experimental Results

Bulk filler versus resonant-cavities– A direct comparison of the two types of baffles was made by measuring the insertion loss of the fiberglass-filled baffles and then removing the fiberglass, changing the perforated skin, modifying the cavity shapes to create configuration C, and repeating the measurements. Figure 7(a) shows that the fiberglass-filled baffles had much the better attenuation (by 5 to 8 dB). However, it was discovered later that configuration C was not representative of a good resonant-cavity design. The cavity shapes in figure 2(a) suggest that the smallest volumes and the tail probably made little contribution to sound attenuation. Configuration E, on the other hand, had five variable-depth cavities on each side, which covered almost the same length of the baffle as those in configuration C and, above 250 Hz, created an insertion loss close to that of the bulk-absorber baffles (fig. 7(b)). It was surprising to find that the frequency response of the two configurations was so similar. Unlike small, single-orifice resonators, the cavities of configuration E had a large number of possible modes and, apparently, did not have the fundamental Helmholtz mode (500 Hz) excited. To maintain a streamlined shape, an acoustically inactive tail was incorporated in configuration E, such that the baffle was 30% longer than the fiberglass baffle, even though the respective acoustic section lengths were similar.

Absorbent liners in cavities– The motivation for the resonant-cavity silencer design was a desire to avoid problems such as erosion and clogging of bulk-absorber silencers. However, it was felt that the all-metallic silencer was not functioning to its potential. Added absorption was needed. It was rationalized that absorbent liners in the cavities would contribute to the sound absorption, yet be far enough removed from the flow to be safe from erosion and clogging. As a result, several liner configurations were evaluated. One was a 25-mm-thick polyurethane foam blanket (32 kg/m^3) attached to the diagonal septa forming the back walls of the cavities (configuration F). Figures 8(a)-8(d) show an improvement in the silencer insertion loss due to the liner of up to 7 dB. It appears that the perforated skin alone did not provide enough acoustic resistance to dissipate the cavity resonances. Even a composite skin (not shown) composed of a screen sandwiched between two perforated plates (same total porosity of 4.5%) did not increase the flow resistance enough to improve the sound absorption. Cavity damping, however, was effective.

Placing a foam liner on the cavity end walls, instead of the diagonal wall (configuration I), also contributed to the attenuation, but not as much as the diagonal wall lining did in the midfrequencies, as shown in figures 9(a) and 9(b).

The best improvement in attenuation was achieved using a 51-mm-thick fiberglass liner (45 kg/m^3) on

[2] Silencer attenuation and insertion loss are different parameters, not necessarily equal; however, for preliminary design purposes the differences can be neglected.

the diagonal septa of a set of baffles (configuration P). Figures 10(a)-10(c) show the large improvement over baffles with unlined cavities, an improvement slightly better than that achieved with the 25-mm foam. However, the 51-mm liner, which filled 25-28% of the cavity, is probably not cost effective, since similar results were achieved with the 25-mm liner that filled 17% of the cavity. It would appear that the thin liner was sufficient to dampen the cavity resonances and thereby reduce the energy available to a second layer of material. This is also evident when the data for the 25-mm foam are compared with data for the fiberglass-filled baffle. To make that comparison, however, the resonant-cavity data had to be extrapolated from a 3.1-m length of cavities to 2.1 m, using results of a following section; this was because the effective acoustic length of the fiberglass baffles was 2.1 m, assuming that only a portion of the tail can be considered acoustically effective. Figure 11 shows that resonant-cavity baffles with 25-mm foam gave a greater insertion loss than comparably sized fiberglass-filled baffles, except at frequencies below 250 Hz, where the fiberglass baffles were consistently superior.

Resonant-cavity shape– Equation (12) indicates that the depth of the baffle cavities affects the impedance and, hence, the silencer insertion loss. However, there is no clue in the theory about cavity length or shape. Work by Lansing and Zorumski (ref. 18) and Zorumski (ref. 19) suggests that duct liner attenuation is enhanced by cavity depths that vary along the silencer length. The sudden changes in impedance should reflect some of the sound back the way it came, as it does in reactive silencers. It was also hoped that making cavities with cross sections more complicated than a rectangle would broaden the frequency response of the silencer by increasing the number of resonant modes. Consequently, various cavity shapes were investigated. As for cavity length, Scharton and Sneddon (ref. 5) suggest that performance can be enhanced by choosing the distance between transverse cavity partitions to be equal to half wavelength of the design peak frequency. This idea has not been checked experimentally.

No data were obtained with baffles composed of all rectangular cavities. However, the insertion loss of baffles with 2 rectangular cavities and 4 triangular cavities (configuration J) is compared with data from baffles with 10 triangular cavities (configuration E) in figures 12(a)-12(d). Although the silencer with rectangular cavities had a fairly broadband attenuation, the attenuation was consistently less than that of the silencer with all triangular cavities. The data show a similar spectrum shape for the two configurations, except at the peak frequency of 315 Hz, where configuration E had considerably more attenuation. Since both configurations had the same porous skin, it is clear that the rectangular cavity was too simple a shape for a good resonant cavity.

Two types of triangular cavities were investigated – one with 10 equal cavities (configuration F) and one with 6 equal cavities and 2 cavities twice as long as the others (configuration G). A comparison of the two types, with foam lining in the cavities, is shown in figures 13(a) and 13(b). The nonuniform cavity volumes enhances the insertion loss of the inlet silencer by approximately 2 dB. Figures 13(c) and 13(d), however, show no clear advantage in the exhaust mode. The reason for this difference between inlet and exhaust is unknown.

To summarize this section, silencer attenuation was enhanced by resonant-cavity cross sections that were triangular rather than rectangular. The effect of cavity number per unit length was not determined.

Baffle length– The effect of baffle length on insertion loss can be inferred from measurements of sound attenuation change along the center passage of the silencer. Figures 14(a) and 14(b) show the attenuation as measured at four stations in the fiberglass silencer, with the acoustic source upstream. Unfortunately, the limited number of measurement points makes the accuracy of the two-slope attenuation curve very uncertain. The double-slope, as explained by Doelling (ref. 14), is due to the rapid attenuation of cross modes in the silencer, followed by a slower attenuation of axially-propagating plane waves. Bullen points out (ref. 20) that curves of sound attenuation through silencers depend not only on the lining properties, but also on the nature of the sound source, since the sound source and duct determine the amount of cross modes present. Because the loudspeaker enclosure was streamwise, the data of figures 14(a) and 14(b) contain a large number of cross modes; the cross modes appear to be absorbed by 1 to 2 m, or 1.5 to 3 duct widths, at a rate between 4 and 8 dB per length equal to duct width.

Much more accurate data were acquired from the resonant-cavity baffles because the attenuation was measured using a traversing microphone, and

the sound source was rotated to give either a maximum or minimum of cross modes in the duct. Figures 15(a) and 15(b) show the sound attenuation through configuration H for four frequencies with the upstream source streamwise. Figures 15(c) and 15(d) show similar data for the upstream source rotated 90° to the duct axis and beaming at the silencer. The low-frequency data have considerable scatter due to floor and ceiling reflections in the passage between the baffles; the reflections were particularly strong with the source beaming parallel to the duct axis (see fig. 15(c)). Consequently, it is difficult to find the true attenuation rate. The data (for 1 kHz and 5 kHz) in figure 15(b) are smooth enough to show the double slope of the curve. In the first 1.5 m (2.5 duct widths) the sound decreased at approximately 3.5 dB per duct width, then decreased at a rate of about 1.5 dB per duct width.

Because of the problems with acoustic reflections in the silencer passages, it was decided that the only definitive way to determine the effect of baffle length was to install and test baffles of various lengths. Figures 16(a)-16(c) show the insertion losses for baffles that were 1.83, 2.44, and 3.05 m long (excluding nose and tail lengths); the lengths are those of configurations O, M, and L, respectively. Those were baffles with 50% duct blockage. Typically, there was a 2 to 3 dB improvement in attenuation, at most frequencies, with each length increase equal to one duct width between baffles (0.61 m).

Baffle thickness– A comparison was made between 305-mm-thick baffles (configuration E) and a similar configuration that was 406 mm thick (configuration L). Figures 17(a)-17(c) show that the 406-mm baffles were typically 2 to 3 dB better above 315 Hz than the 305-mm baffles. The comparison is confused somewhat, because the 305-mm baffles blocked 40% of the duct, and the 406-mm baffles blocked 50% of the duct. The respective baffle passage widths were 610 mm and 508 mm. It is not clear how much of the improved attenuation was due to deeper cavities and how much was due to narrower passages between the baffles. What is needed is a set of data showing the independent effects of baffle thickness and blockage along with the respective pressure drop data, since it is pressure drop data that limit the allowable duct blockage. In a later section, pressure drop data from the baffles that were 305 mm and 406 mm thick are discussed.

Perforated skin porosity– The analytical phase of the study showed that low-porosity perforated skins would be required to achieve adequate acoustic resistance and absorption, and that a 2% to 5% porosity would be optimum for the maximum flow speed of 31 m/sec between the baffles. Consequently, two skin porosities were evaluated: open areas of 2.6% and 4.9%. A comparison of the resulting insertion loss is shown in figures 18(a)-18(c). The two configurations had different plate thicknesses, but, as will be shown, plate thickness is a weak parameter. The data show that in most cases the 4.9% porosity gave slightly better insertion loss than the 2.6% porosity.

Perforated skin thickness– Equations (6) and (10) indicate that the skin thickness has an effect on the resistance and reactance of the resonant-cavity impedance. However, doubling the thickness did not have an appreciable effect on silencer insertion loss analytically or experimentally. Figures 19(a)-19(c) show that, if anything, the measured insertion loss for the inlet simulation was improved 1 or 2 dB by the thicker material. The differences, however, were generally less than the accuracy limits of the data.

Wind effects– Typical insertion-loss data with upstream and downstream sound propagation are illustrated in figures 20(a) and 20(b). The flow speeds were dissimilar but the effects are clear. Attenuation of sound propagating upstream is diminished a few dB at midfrequencies to high frequencies relative to the zero wind case (fig. 20(a)). The opposite was true for downstream propagation of sound, that is, an increase of midfrequency to high-frequency sound attenuation (fig. 20(b)). These effects are consistent with the idea of sound refraction in a flow with a velocity gradient (ref. 21). Because of friction at the baffle surface, the flow velocities are higher in the passage center than near the baffles. Thus, sound waves moving upstream would tend to refract away from the walls resulting in a decrease of insertion loss, and waves traveling downstream would refract into the baffles causing an increase of insertion loss. The low-frequency sound is less sensitive to these refraction effects because the wavelengths are long compared to the velocity gradient region. The results are contrary to those of Kurze and Allen (ref. 22), who found that sound propagating upstream in a very small duct (25.4 mm × 25.4 mm) was attenuated by the flow,

presumably because of the increased interaction time between the waves and duct lining. Apparently, the effect of wind depends on the relative size of the duct and wavelengths.

Flow-induced tones– Under certain conditions, flow over the undamped baffles created loud tones, owing to pressure resonances that would obliterate the effectiveness of the silencer if allowed to exist. Thus the title of this paper is somewhat misleading because it is essential that the silencer cavities *not* resonate freely. The term "resonant-cavity baffle" was chosen because of our familiarity with the Helmholtz resonator, a device that also must be prevented from resonating freely if sound is to be absorbed rather than generated.

Tsui and Flandro (ref. 23) found that cavities covered by perforated plates will sing if vortex shedding in the perforate holes couples with cavity- or duct-pressure resonances. Their data suggested a vortex shedding rate that varied with flow speed and perforate hole diameter as follows:

$$f = \frac{StU}{a} \tag{14}$$

where the Strouhal number St was also a function of hole diameter a (in millimeters):

$$St = 0.02\,a + 0.15 \tag{15}$$

for the range $2 \leqslant a \leqslant 10$ mm. As an example of flow-induced tones, figures 21(a)–21(c) illustrate the acoustic spectra measured by microphone 2 (upstream) with configuration N, a particularly noisy configuration, operated at three flow speeds. The peak tones stood 40 dB above the broadband noise. The calculated vortex shedding and measured peak tone frequencies are:

U, m/sec	f calculated, Hz (eq. (14))	f measured, Hz (fig. 21)
23	1525	1600
37	2425	2475
44	2900	3250

The agreement is good considering that the actual flow speeds near the baffle surface were not measured. The flow speeds listed on the figures were computed using the measured dynamic pressure upstream of the baffles and the relative areas of the duct and baffle passages. Undoubtedly, the speed varied over the cavities because of flow accelerations over the baffle noses and decelerations along the tails, which would account for some of the multiple tones in figures 21(a)–21(c). In other words, different cavities may have had different modes excited because of variations in flow speed on the surface.

The onset of flow-induced tones occurred at frequencies well above the fundamental Helmholtz frequency. Figure 22 shows three configurations (A, C, and D) and the flow speeds at which the tones were first detected as well as the speeds at which higher modes cut in. As the flow speed increased, the tonal frequencies would remain fairly steady until the vortex shedding was able to decouple from the cavity resonance and jump to a higher frequency corresponding to a higher cavity mode, where coupling again occurred. The fundamental Helmholtz frequency is given by (ref. 24):

$$f = \frac{c}{2\pi}\left(\frac{S}{\ell V}\right)^{1/2} \tag{16}$$

where

c = sound speed

S = area of all holes over cavity

V = cavity volume

$\ell = t + \delta$

t = plate thickness

$\delta = 0.85\,a$

a = hole diameter

For configuration A, the Helmholtz frequency is 505 Hz, whereas the first tone was detected in the 2500-Hz third-octave band. Without cavity pressure measurements, it is not clear if the cavity depth mode or transverse mode was excited; however, from the sequence of frequencies listed in figure 22, the most likely choice is the quarter-wave depth mode given by (ref. 24):

$$f = (2n - 1)\,\frac{c}{4d} \tag{17}$$

where

n = mode number 1, 2, 3, . . .

d = cavity depth

The first audible tone from configuration A corresponds to the third mode (n = 3) given by equation (17). Presumably, the Helmholtz mode was not excited because the necessary flow speed of 4 m/sec (from eq. (14)) was two low for the generation of sufficiently strong vortices.

Figure 22 also shows that the more complicated cavity shapes could be driven to higher speeds before cavity resonance was detected. Not shown are the effects of perforate-hole geometry. It was observed, for example, that configurations with 3.2-mm-diam holes generated louder tones than those with 1.6-mm holes; and one hole pattern, 1.6-mm-diam holes on 6.4-mm centers, did not excite cavity resonance at the flow speeds used. This phenomenon will be studied further.

How can flow-induced tones be eliminated? One way is to install absorbent liners in the cavities. This is illustrated in figure 23, which shows the acoustic spectra of configuration A with and without a 51-mm foam lining in the cavities. The lining eliminated the tone.

This also indicates that there were no resonances in the passages between the baffles like those observed by Tsui and Flandro (ref. 23) in their small 76- by 76-mm duct. However, two configurations that had solid panels under the perforated skin on portions of the baffle surface (configurations J and K) did generate duct resonances. Figure 24 illustrates the tone created by configuration K despite the acoustic lining in the rectangular cavities. It was confirmed later that the triangular cavities were not resonating. The resonances could only be eliminated by perturbing the flow between the baffles with a bluff body or by attaching foam blankets to the *outer* surface of the baffles. Even though the solid panels were staggered such that no two faced each other across the passage, strong duct resonances were created. This type of configuration should be avoided. Duct resonances were not created by baffles with only 2.6% open-area surfaces, even when cavity resonances were generated.

To conclude this section, flow-induced tones from undamped baffles are sufficiently worrisome and unpredictable that a designer should either add a thin absorbent liner to the cavities or confirm experimentally that his design does not generate loud tones.

Inlet versus exhaust– There was no great advantage to using the baffles in the inlet or exhaust mode. However, much of the data showed slightly better attenuation for the inlet configuration in the mid-frequency and high-frequency range, as shown typically in figure 25. Presumably, the baffle tails rejected some of the sound that the baffle noses did not.

Effect of acoustic field– As mentioned several times in this report, the silencer performance was dependent on the orientation of the acoustic source and, hence, on the nature of the acoustic field at the silencer entrance. Figures 26(a) and 26(b) illustrate the approximately 6 dB drop in insertion loss at midfrequencies and high frequencies resulting from the change of source orientations from streamwise to perpendicular to the duct. The streamwise source generated a more reverberant field than did the perpendicular source. With the source perpendicular to the duct and beaming along the duct axis, a portion of the smaller wavelength sound propagated straight through the silencer passages. Similar results were observed for the fiberglass-filled silencer. This type of sound field can best be trapped by increasing the blockage or by adding baffles that block the line of sight through the silencer. Savkar et al. proposed a novel ideal for this problem (ref. 25); they suggested that it may be feasible, in some cases, to introduce aerodynamic bodies in the silencer passages that skew the flow and thereby enhance the refraction of the acoustic energy into the lining. In any case, figures 26(a) and 26(b) illustrate the need for some knowledge of the expected sound field before published silencer data are applied to a specific problem.

Mylar membrane in fiberglass baffles– An obvious way to protect fiberglass filler from erosion and moisture absorption is to place a plastic membrane between the fiberglass and metallic covering. To evaluate the acoustic effects of such a configuration, we installed a 0.025-mm-thick Mylar membrane between the fiberglass and perforated skin of the configuration shown in figure 1(c). The fiberglass had to be squeezed into the baffles, which pushed the membrane into the perforations. The resulting degradation of sound attenuation was substantial, as shown in figure 27. In a solution to this problem

described by Bender et al. (ref. 26), the membrane is sandwiched between plastic meshes, and the sound absorption is actually improved below 2 kHz compared with the case of fiberglass alone. The procedure was not attempted in this study.

Pressure drop– The measurement of pressure drop across the silencer was complicated by the fact that the baffle trailing edges were just upstream of the wind-tunnel diffuser, which is a region of pressure change. (The pressure drop measurements were made by William T. Eckert of Aeromechanics Laboratory, U.S. Army Research and Technology Laboratory, Ames Research Center, Moffett Field, California). By measuring the streamwise static pressure distribution from 1 chord upstream to 3.5 chords downstream of the silencer with and without the baffles installed, the change in static pressure across the silencer was determined. Figure 28 shows a typical plot of static pressure variation through silencer configuration L. Actually, the total pressure loss is the more common parameter, which, from Bernoulli's law, is equal to the change in static pressure. Figure 29 shows the silencer pressure drop for several configurations normalized by the free-stream dynamic pressure q_o, measured upstream of the baffles. Data scatter is shown by vertical lines through the data. Increasing the duct blockage percentage from 40% to 50% (305-mm to 406-mm baffles) tripled the pressure drop. Increasing the baffle length from 3.1 m to 4.3 m caused the pressure drop to increase approximately 22%. Finally, it was observed that porous tail skins containing fiberglass filler created more pressure drop than solid skin tails.

Predicting silencer pressure drop is difficult. Mechel (ref. 4) described a simple empirical method that can be used to estimate the pressure loss of parallel baffles as follows:

$$\frac{\Delta P}{q_1} = k_1 \frac{b/h}{1 + b/h} + k_2 \frac{\ell}{2h} + k_3 \left(\frac{b/h}{1 + b/h} \right)^2 \tag{18}$$

where

ΔP = total pressure drop

q_1 = dynamic pressure between baffles

b = half baffle thickness

h = half distance between baffles

k_1 = 0.05 for round leading edge

k_2 = $2.5(10)^{-3}$, friction factor for perforated metal sheet

k_3 = 0.6 for tail angles 6° from streamwise

Using equation (18) for the configurations of figure 29, and adjusting for the free-stream dynamic pressure, resulted in the values of normalized pressure drop shown in table 1. Mechel's method was intended for fiber-filled baffles, but even in that case the predicted pressure loss was 48% below the measured value. Perhaps the empirical model was too simple, or perhaps the friction factors should be adjusted for Reynolds number and surface roughness. Eckert et al. (ref. 26) have published a much more elaborate method that has been incorporated in a computer code because of the number of parameters and equations involved. Their method will give reasonably good accuracy for silencer pressure drop, if the user can determine the value of friction factors appropriate for his design, a difficult task in many cases.

TABLE 1.– A COMPARISON OF PREDICTED AND MEASURED VALUES OF NORMALIZED PRESSURE DROP

Configuration	$\Delta P/q_o$	
	Predicted (eq. (18))	Measured (fig. 29)
Fiberglass baffles with porous tail	0.27	0.52
Resonant cavity baffles		
O	0.43	1.18
M	0.44	1.39
L	0.45	1.62

CONCLUSIONS

An analytical and experimental study of resonant-cavity, parallel baffles has shown that a duct silencer composed of these baffles had acoustical performance similar to a silencer composed of fiberglass-filled baffles. A method for predicting silencer attenuation is described. The primary conclusions of the study are based on measurements of silencer insertion loss in the 7- by 10-Foot Wind Tunnel at Ames Research Center. Evaluations of several important parameters have shown the following.

1. The attenuation of undamped, resonant-cavity baffles covered a broad frequency range.

2. The addition of 25-mm-thick foam liners to 305-mm-deep cavities improved the attenuation substantially. Above 250 Hz, the resulting insertion loss was equal to or somewhat better than that of a fiberglass-filled silencer of comparable size.

3. Many of the undamped, resonant-cavity configurations generated loud cavity tones, which could be eliminated by adding sound-absorbent material to the cavities. Rectangular cavities generated tones at lower speeds than triangular cavities.

4. Duct-resonance tones were created by configurations that had solid surfaces flush with the airflow. This type of configuration should be avoided.

5. The resonant-cavity baffle attenuation depended on cavity shape. A series of variable-depth cavities with triangular cross sections in each baffle gave better attenuation than constant-depth, rectangular cross-section cavities.

6. The 406-mm-thick resonant-cavity baffles were tested at three lengths. There was 2 to 3 dB improvement in attenuation for each increase in length that was equal to one duct width between baffles.

7. Increasing duct blockage from 40% to 50% by increasing baffle thickness improved the insertion loss by 2 to 3 dB. However, the effects of blockage and baffle thickness were not separated.

8. Of the two skin porosities evaluated for the resonant-cavity baffles, the 2.6%-open-area skins gave somewhat better attenuation at low frequencies, and the 4.9%-open-area skins gave somewhat better attenuation at midfrequencies and high frequencies.

9. The directivity of the source had a strong effect on silencer performance. At midfrequencies to high frequencies the insertion loss was typically 5 to 10 dB greater when the source was beaming at the duct walls compared with that when the source was beaming along the duct axis. The first situation had many more cross modes for the silencer to absorb than did the second.

10. In the inlet mode, sound propagation against the wind caused a reduction of attenuation in the midfrequency to high-frequency range compared with the zero wind case. In the exhaust mode, the reverse was true; that is, sound propagation with the wind caused an increase in the midfrequency to high-frequency attenuation.

11. A 0.025-mm-thick Mylar membrane between the fiberglass and perforated skin had a very deleterious effect on attenuation of the fiberglass baffles.

12. The pressure drop of the silencers normalized by free-stream dynamic pressure ranged from 0.34 to 1.62, depending on duct blockage, baffle length, and baffle type. The strongest parameter was blockage. Increasing duct blockage from 40% to 50% caused the pressure drop to triple. Increasing the baffle length from 3.1 m to 4.3 m caused the pressure drop to increase approximately 22%. The pressure drop of the fiberglass baffles increased from 0.34 to 0.51 when a smooth tail skin was replaced by a perforated skin. The silencer pressure drop was 2 to 3.5 times higher than calculated using an empirical prediction method.

Ames Research Center
National Aeronautics and Space Administration
and
Aeromechanics Laboratory
AVRADCOM Research and Technology Laboratories
Ames Research Center, Moffett Field, California 94035, December 1, 1980

REFERENCES

1. Mort, Kenneth W.; Soderman, Paul T.; and Eckert, William T.: Improving Large-Scale Testing Capability by Modifying the 40- by 80-Foot Wind Tunnel. J. Aircraft, vol. 16, no. 8, Aug. 1979, pp. 571-575 (also AIAA Paper 77-587, June 1977).
2. Soderman, Paul T.; and Page, V. R.: Acoustic Performance of Two 1.83-Meter-Diameter Fans Designed for a Wind Tunnel Drive System. NASA TP-1008, 1977.
3. Scharton, T. D.; Sawley, R. J.; and Wilby, E. G.: An Acoustic Study for the Modified 40- by 80-Foot Wind Tunnel. BBN Report 2765, Feb. 1975 (NASA Contract NAS2-8330).
4. Mechel, F. P.: Design Criteria for Industrial Mufflers. Inter-Noise 75 Proceedings, Sendai, Japan, 1975, pp. 751-760.
5. Scharton, T. D.; and Sneddon, M. T.: Acoustical Properties of Materials and Muffler Configurations for the 80- by 120-Foot Wind Tunnel. NASA CR-152065, 1977 (also BBN Report 3563).
6. Soderman, P. T.: Design and Performance of Resonant-Cavity Parallel Baffles for Duct Silencing. Noise Control Engineering, vol. 17, no. 1, 1981, pp. 12-21.
7. Soderman, P. T.; and Scharton, T. D.: All-Metal Muffler for Ducts. ARC-11159, NASA Tech Briefs, vol. 4, no. 2, summer 1979, p. 275.
8. Peterson, Arnold P. G.; and Gross, E. E.: Handbook of Noise Measurement. Sixth ed., General Radio Company, West Concord, Mass., 1967.
9. Schultz, T. J.: Wrappings, Enclosures and Duct Linings. Noise and Vibration Control, Leo L. Beranek, ed., McGraw-Hill Book Company, 1971, pp. 502-511.
10. Doelling, Norman; and Bolt, Richard H.: Noise Control for Aircraft Engine Test Cells and Ground Run-Up Suppressors. Vol. 2: Design and Planning for Noise Control. WADC Technical Report 58-202(2), Nov. 1961.
11. Trebble, W. J. G.: Exploratory Studies on the Design of Acoustic Splitters for Wind Tunnels. RAE Tech. Memo Aero. 1829, Jan. 1980.
12. Kurze, U.: Schallausbreitung im Kanal mit periodischer Wandstruktur (Sound Propagation in a Duct of Periodic Wall Structure). Acustica, vol. 21, 1969, pp. 74-85.
13. Ingard, U.; and Ising, H.: Acoustic Nonlinearity of an Orifice. JASA, vol. 42, no. 1, July 1967, pp. 6-17.
14. Doelling, N.: Dissipative Mufflers. Noise Reduction, Leo L. Beranek, ed., McGraw-Hill Book Company, 1960, ch. 17.
15. Baumeister, Kenneth J.; and Rice, Edward J.: Visual Study of the Effect of Grazing Flow on the Oscillatory Flow in a Resonator Orifice. NASA TM X-3288, 1975.
16. Rogers, T.; and Hersh, A. S.: The Effect of Grazing Flow on the Steady State Resistance of Square-Edged Orifices. AIAA Paper 75-493, Mar. 1975.
17. Rice, E. J.: A Theoretical Study of the Acoustic Impedance of Orifices in the Presence of a Steady Grazing Flow. NASA TM X-71903, 1976.
18. Lansing, D. L.; and Zorumski, W. E.: Effects of Wall Admittance Changes on Duct Transmission and Radiation of Sound. J. Sound Vib., vol. 27, no. 1, Mar. 8, 1973, pp. 85-100.
19. Zorumski, W. E.: Noise Suppressor, U.S. Patent 3,830,335, Aug. 1974.
20. Bullen, R.: To-The-Editor. Noise Control Engineering, vol. 8, no. 1, Jan.-Feb. 1977, pp. 3-4.
21. Hirschorn, M.: The Aeroacoustic Rating of Silencers for Forward and Reverse Flow of Air and Sound. Noise Control Engineering, vol. 2, no. 1, 1974, pp. 25-29.
22. Kurze, U. J.; and Allen, C. H.: Influence of Flow and High Sound Levels on the Attenuation in a Lined Duct. JASA, vol. 49, no. 5 (part 2), 1971, pp. 1643-1654.
23. Tsui, C. Y.; and Flandro, G. A.: Self-Induced Sound Generation by Flow Over Perforated Duct Liners. J. Sound Vib., vol. 50, no. 3, Feb. 1977, pp. 315-332.
24. Kinsler, Lawrence E.; and Frey, Austin R.: Fundamentals of Acoustics. Second ed., John Wiley & Sons, 1962.

25. Savkar, S. D.; Hehmann, H. W.; and Motsinger, R. E.: Refractive Enhancement of a Flow Duct Liner Performance. J. Sound Vib., vol. 38, no. 3, Feb. 8, 1975, pp. 414-416.
26. Bender, Erich K.; Patterson, William N.; and Kaye, Michael C.: Truck Noise. III-C. Source Analysis and Experiments with Noise Control Treatment Applied to Freightliner Quieted Truck. Report DOT-TST-74-20, Department of Transportation, Washington, D.C., Jan. 1974.
27. Eckert, William T.; Mort, K. W.; and Jope, Jean: Aerodynamic Design Guidelines and Computer Program for Estimation of Subsonic Wind Tunnel Performance. NASA TN D-8243, 1976.

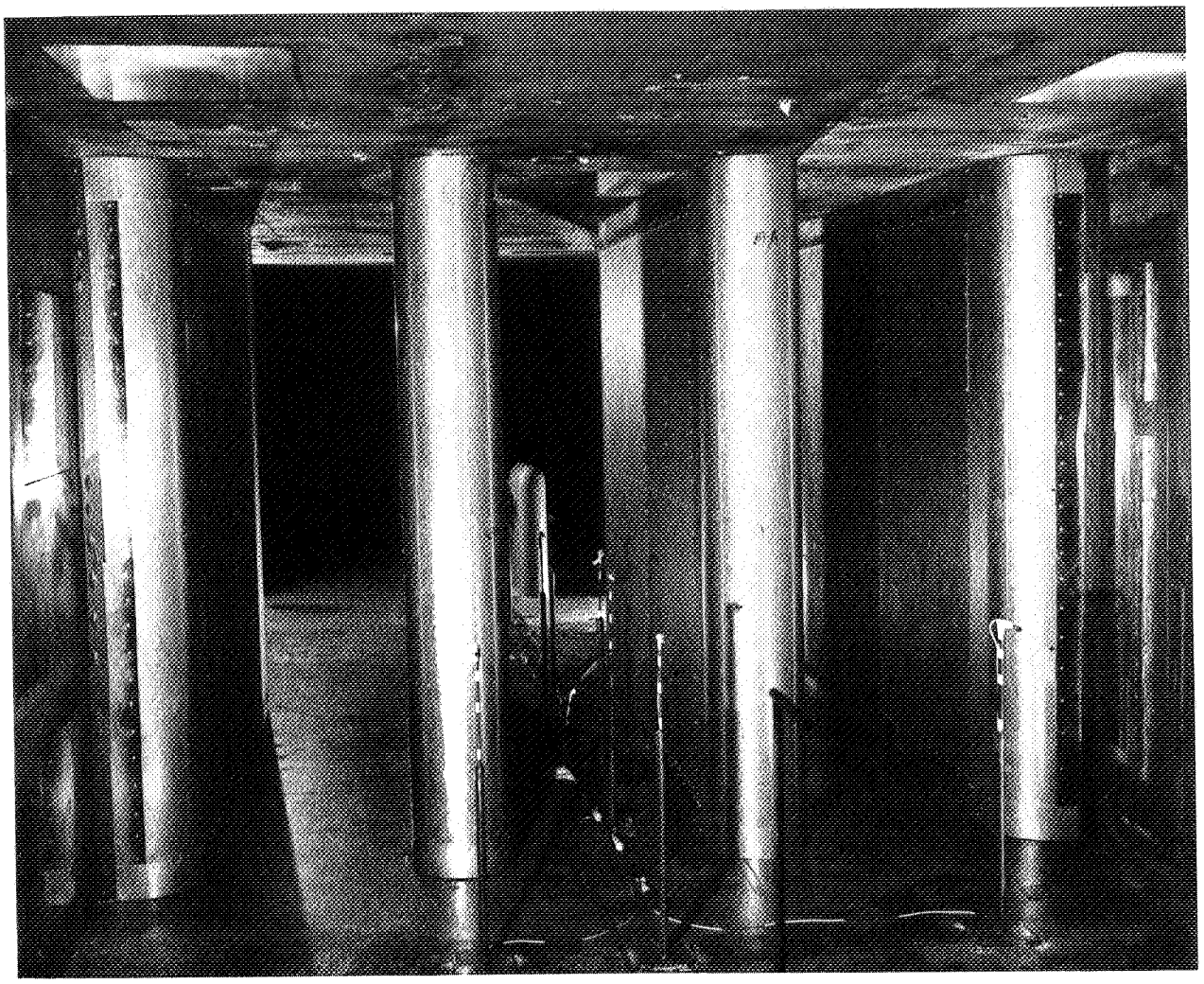

(a) Looking downstream.

Figure 1.– Fiberglass-filled baffles in the wind tunnel.

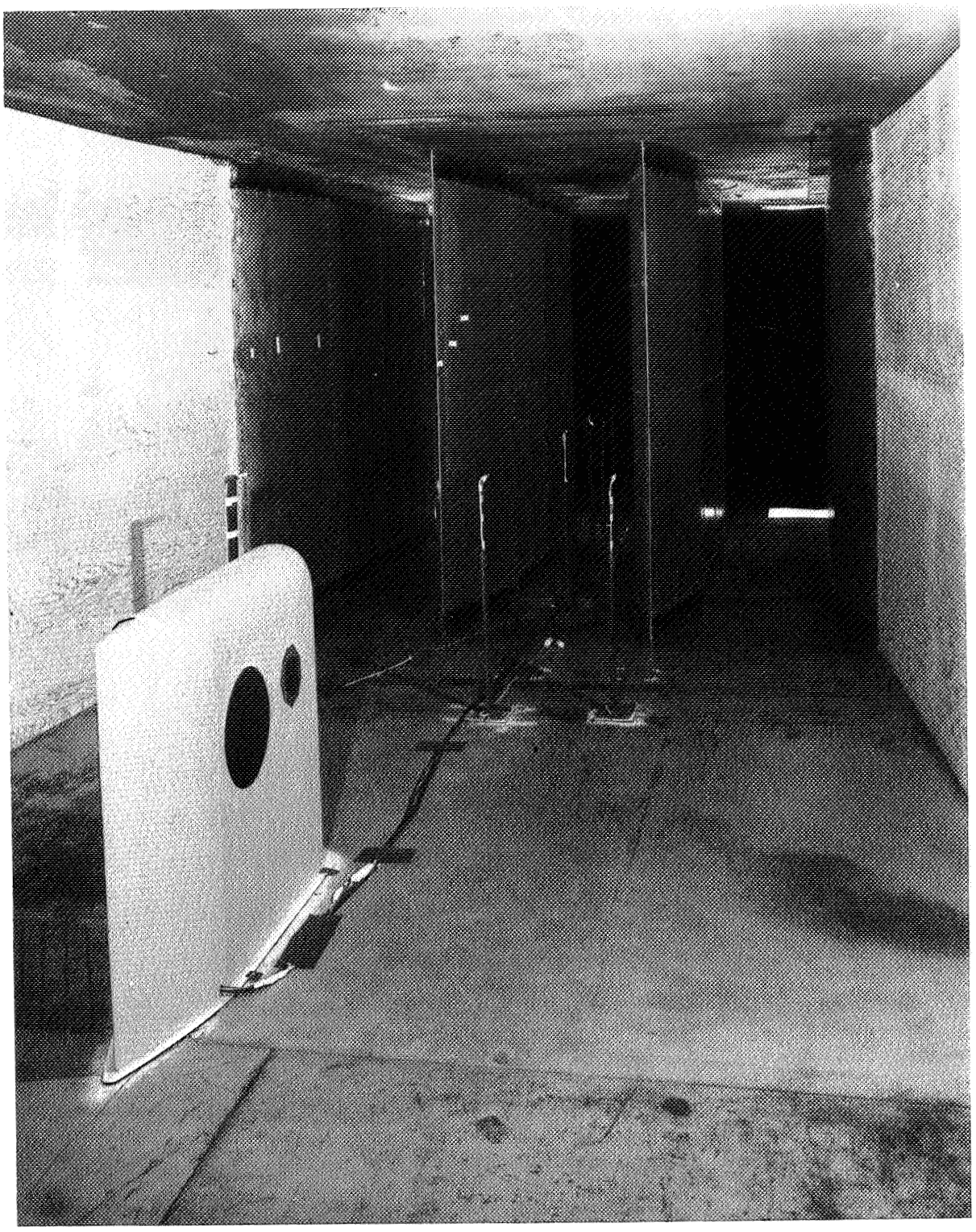

(b) Looking upstream.

Figure 1.– Continued.

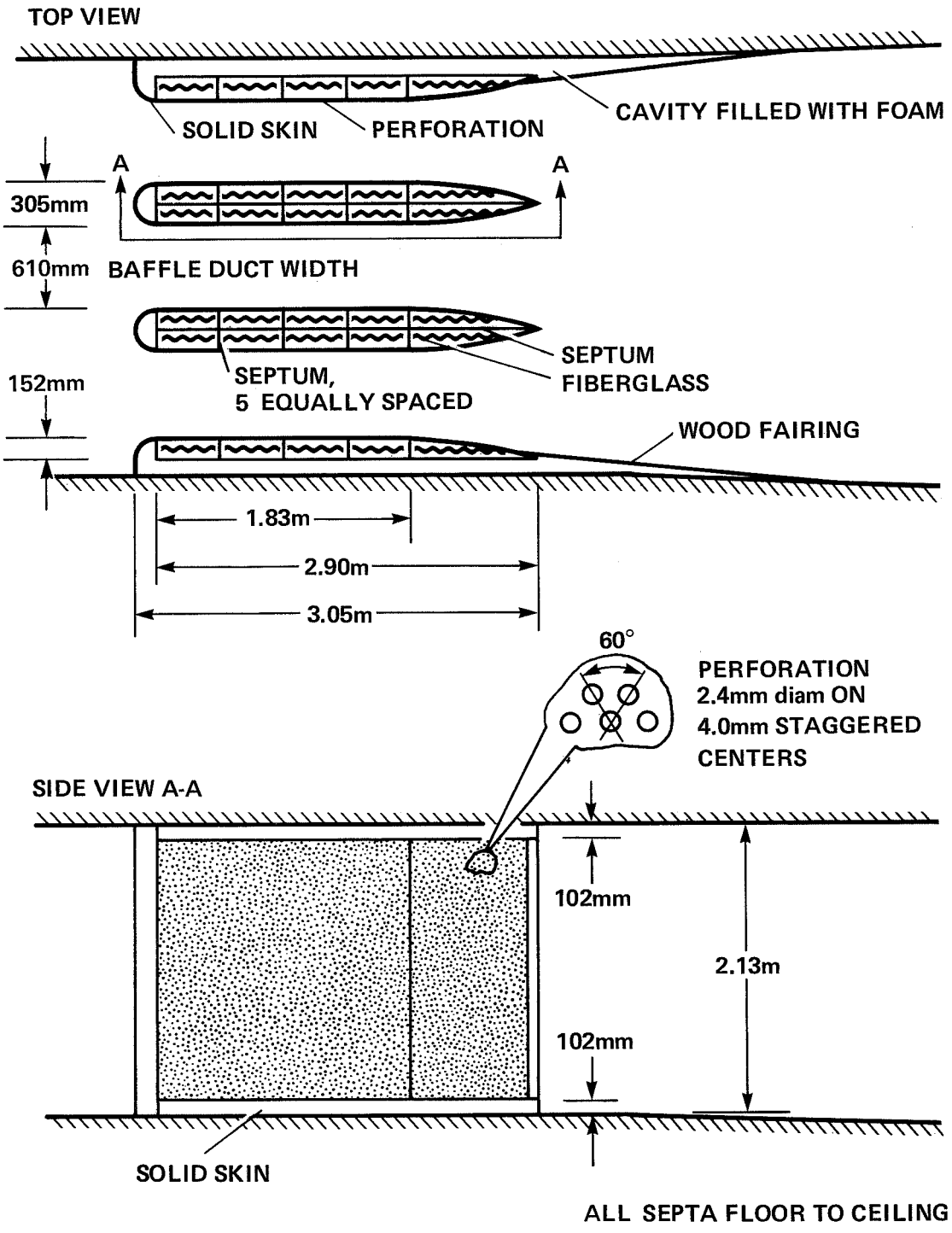

(c) Dimensions.

Figure 1.– Concluded.

CONFIG	HOLE SIZE, mm	HOLE SPACING, mm	POROSITY, %	HOLE PATTERN*	SKIN THICKNESS, mm	CAVITY LINER
A 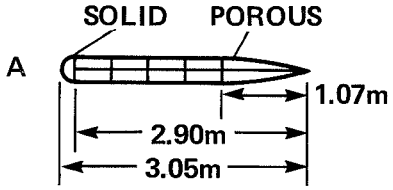	1.6	8.7	2.6	STRAIGHT	0.61	NO
B 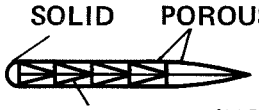 URETHANE FOAM (NO METAL SEPTA ON DIAGONAL) 45 kg/m^3, 51mm THICK	1.6	8.7	2.6	STRAIGHT	0.61	YES
C 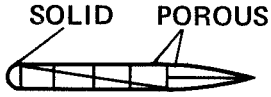	1.6	8.7	2.6	STRAIGHT	0.61	NO
D 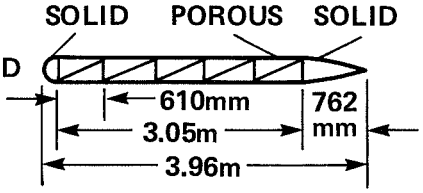	1.6	8.7	2.6	STRAIGHT	0.61	NO

*STRAIGHT STAGGERED

ALL BAFFLES 305 mm THICK
ALL CAVITIES EMPTY EXCEPT FOR LINERS
ALL SEPTA RUN HEIGHT OF BAFFLES

(a) Configurations A-D.

Figure 2.– Resonant-cavity baffle geometries.

CONFIG	HOLE SIZE, mm	HOLE SPACING, mm	POROSITY, %	HOLE PATTERN	SKIN THICKNESS, mm	CAVITY LINER
E 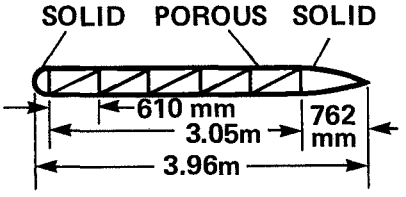	1.6	6.4	4.9	STRAIGHT	1.2	NO
F  URETHANE FOAM ON SEPTA 32 kg/m^3, 25mm THICK	1.6	6.4	4.9	STRAIGHT	1.2	YES
G 	1.6	6.4	4.9	STRAIGHT	1.2	YES
H SAME AS G WITH 0.61 mm THICK SKIN						SAME AS F
I  URETHANE FOAM ON SEPTA 32kg/m^3, 25mm THICK	1.6	6.4	4.9	STRAIGHT	0.61	YES
J 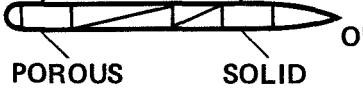	1.6 OR 3.2	6.4 12.7	4.9 4.9	STRAIGHT STRAIGHT	0.61 0.91	NO NO
K 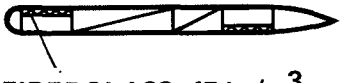 FIBERGLASS, 45 kg/m^3, 51mm THICK COVERED BY POLYESTER CLOTH	3.2	12.7	4.9	STRAIGHT	0.61	YES
ALL BAFFLES 305 mm THICK						

(b) Configurations E-K.

Figure 2.– Continued.

CONFIG	HOLE SIZE, mm	HOLE SPACING, mm	POROSITY, %	HOLE PATTERN	SKIN THICKNESS, mm	CAVITY LINER
L 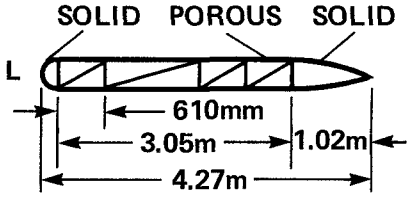	1.6	6.4	4.9	STAGGERED	0.61	NO
M 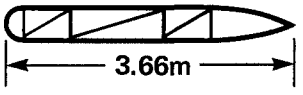	1.6	6.4	4.9	STAGGERED	0.61	NO
N 	3.2	12.7	4.9	STRAIGHT	0.61	NO
O 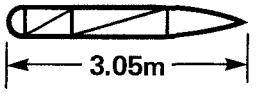	1.6	6.4	4.9	STAGGERED	0.61	NO
P 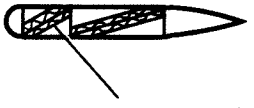	1.6	6.4	4.9	STAGGERED	0.61	YES
	ALL BAFFLES 406 mm THICK					

(c) Configurations L-P.

Figure 2.– Concluded.

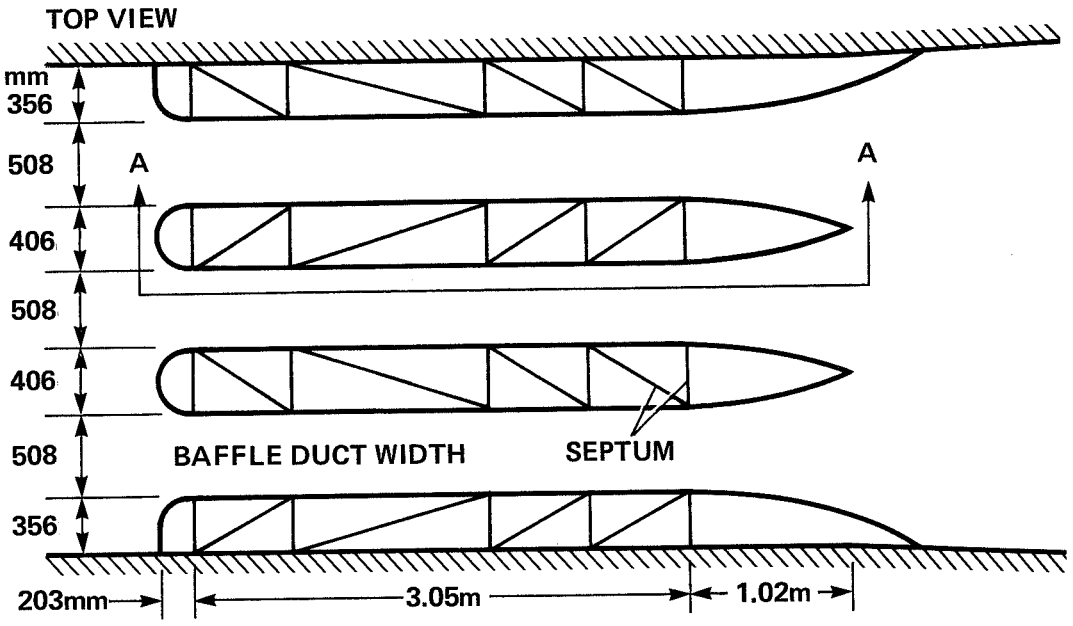

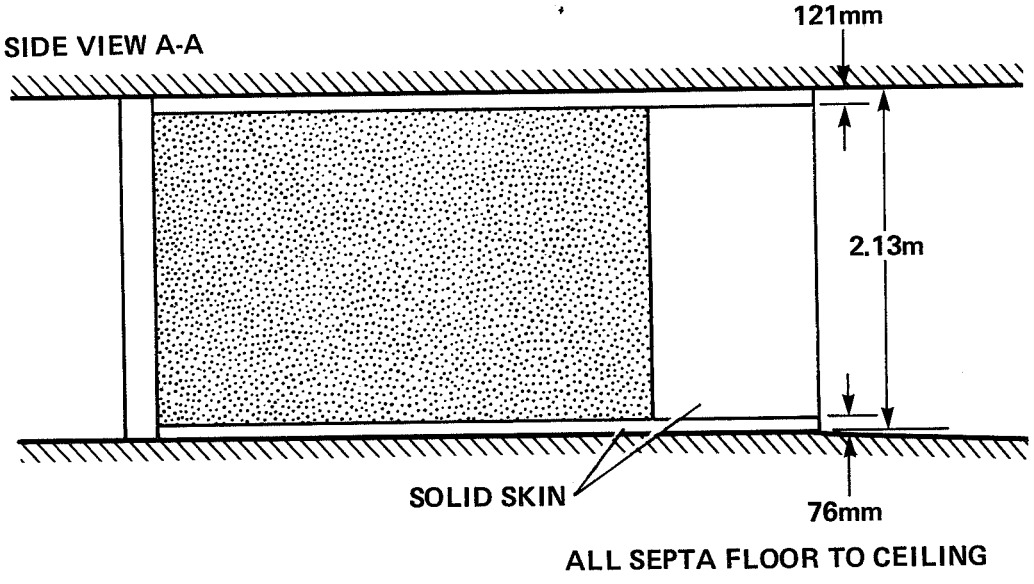

Figure 3.– Schematic of resonant-cavity configuration L.

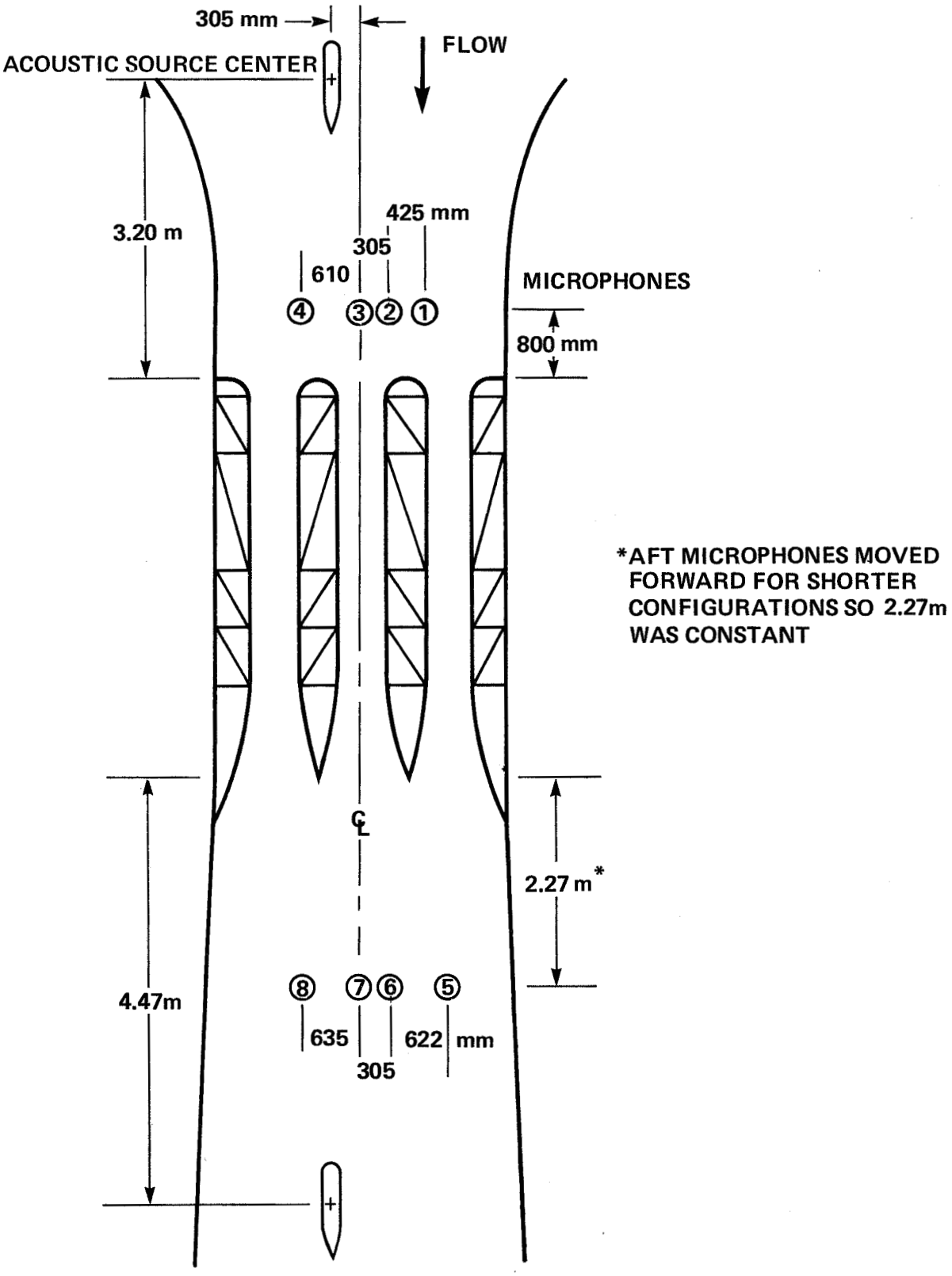

(a) Microphone locations.

Figure 4.– Microphone location and instrumentation.

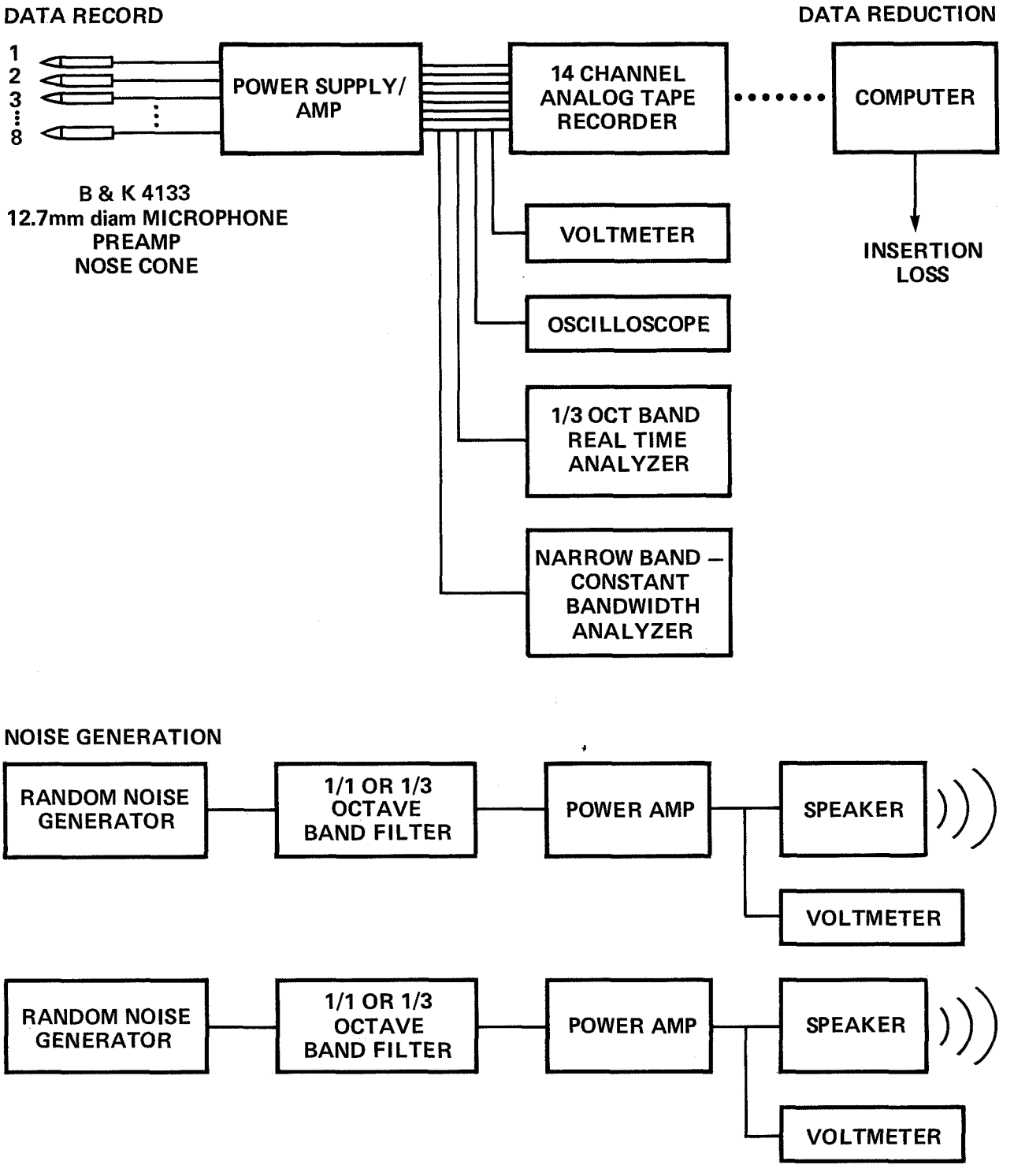

(b) System schematic.

Figure 4.– Concluded.

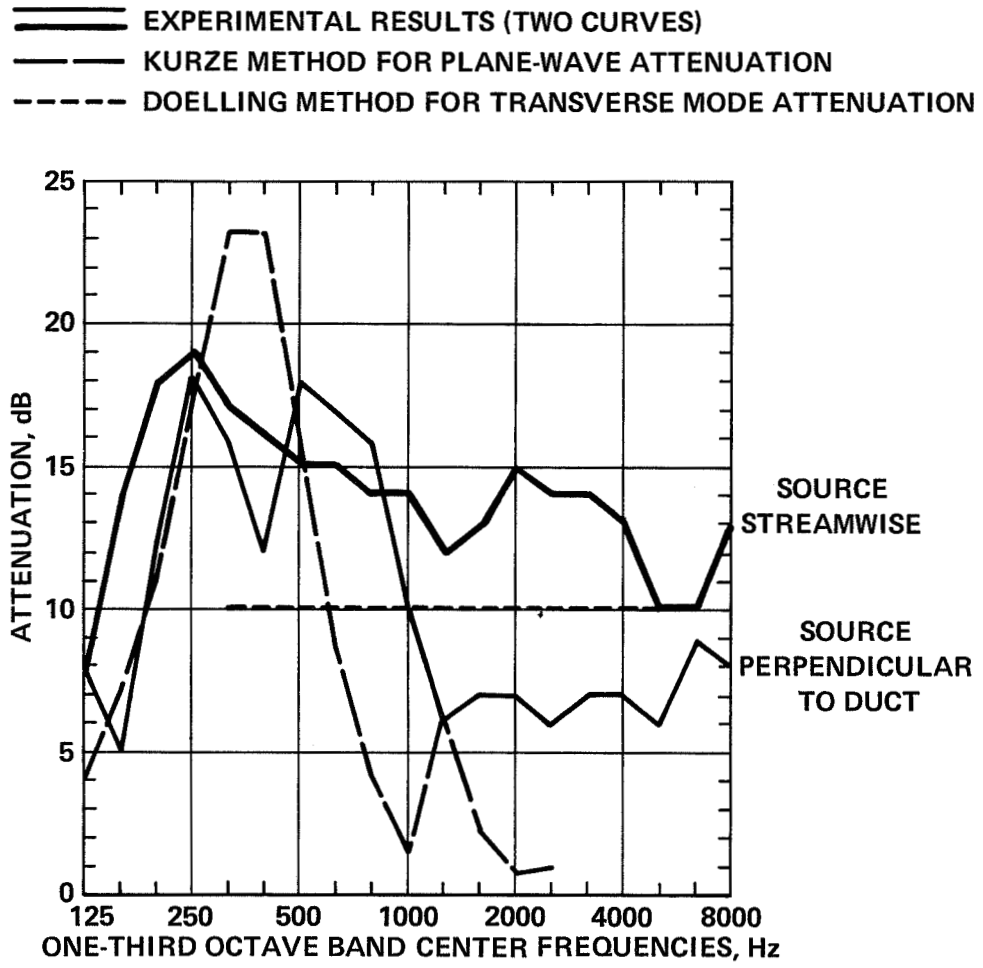

Figure 5.– Fiberglass silencer performance – analytical and experimental: $U = 0$, exhaust simulation.

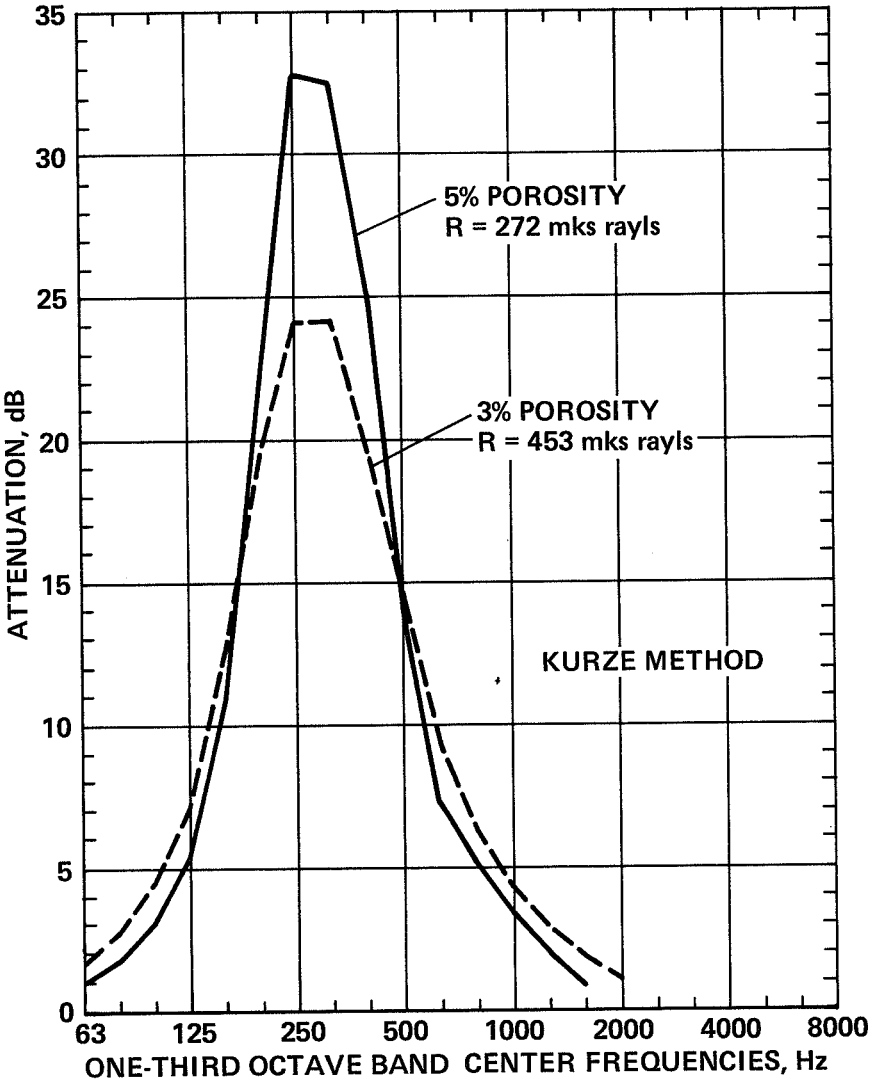

(a) $U = 17$ m/sec.

Figure 6.– Resonant-cavity silencer performance – analytical and experimental, configuration D.

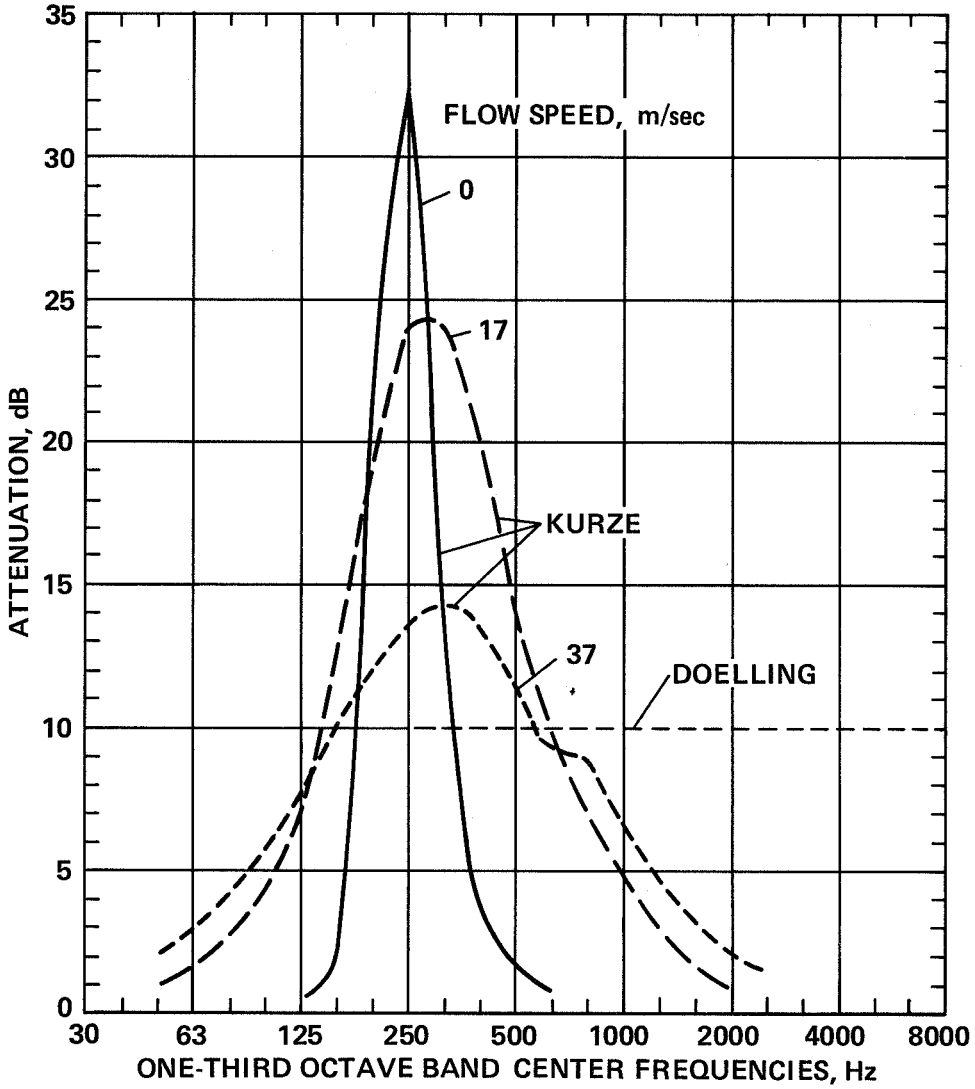

(b) 3% porosity, variable wind speed.

Figure 6.– Continued.

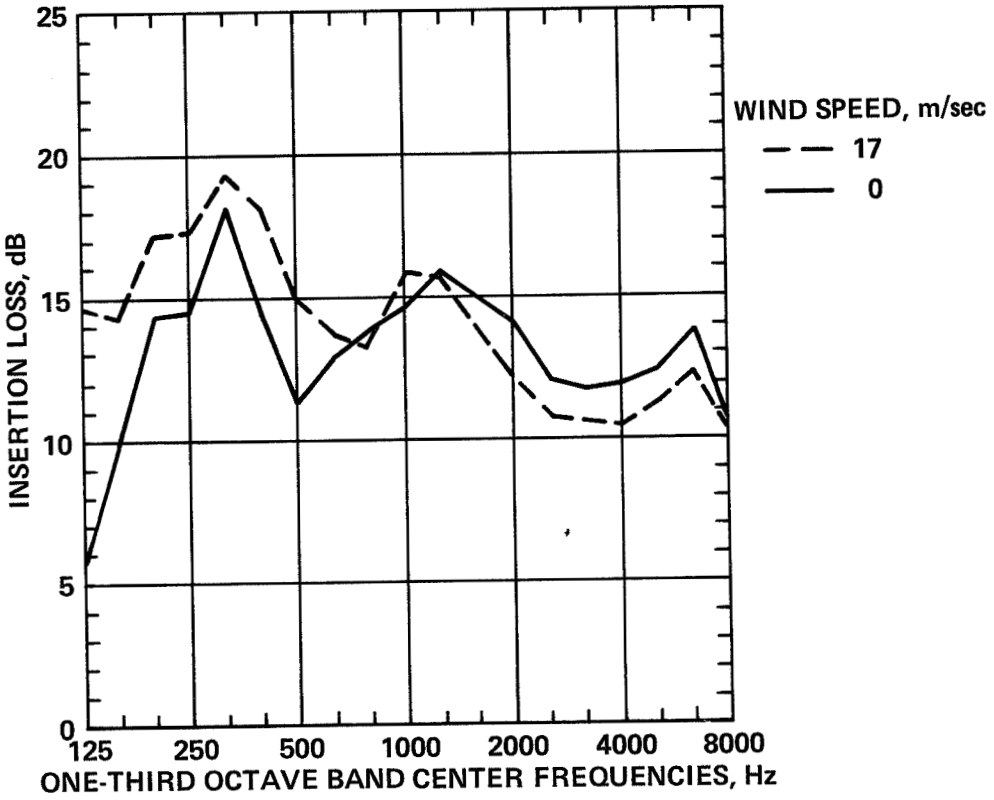

(c) Measured results.

Figure 6.– Concluded.

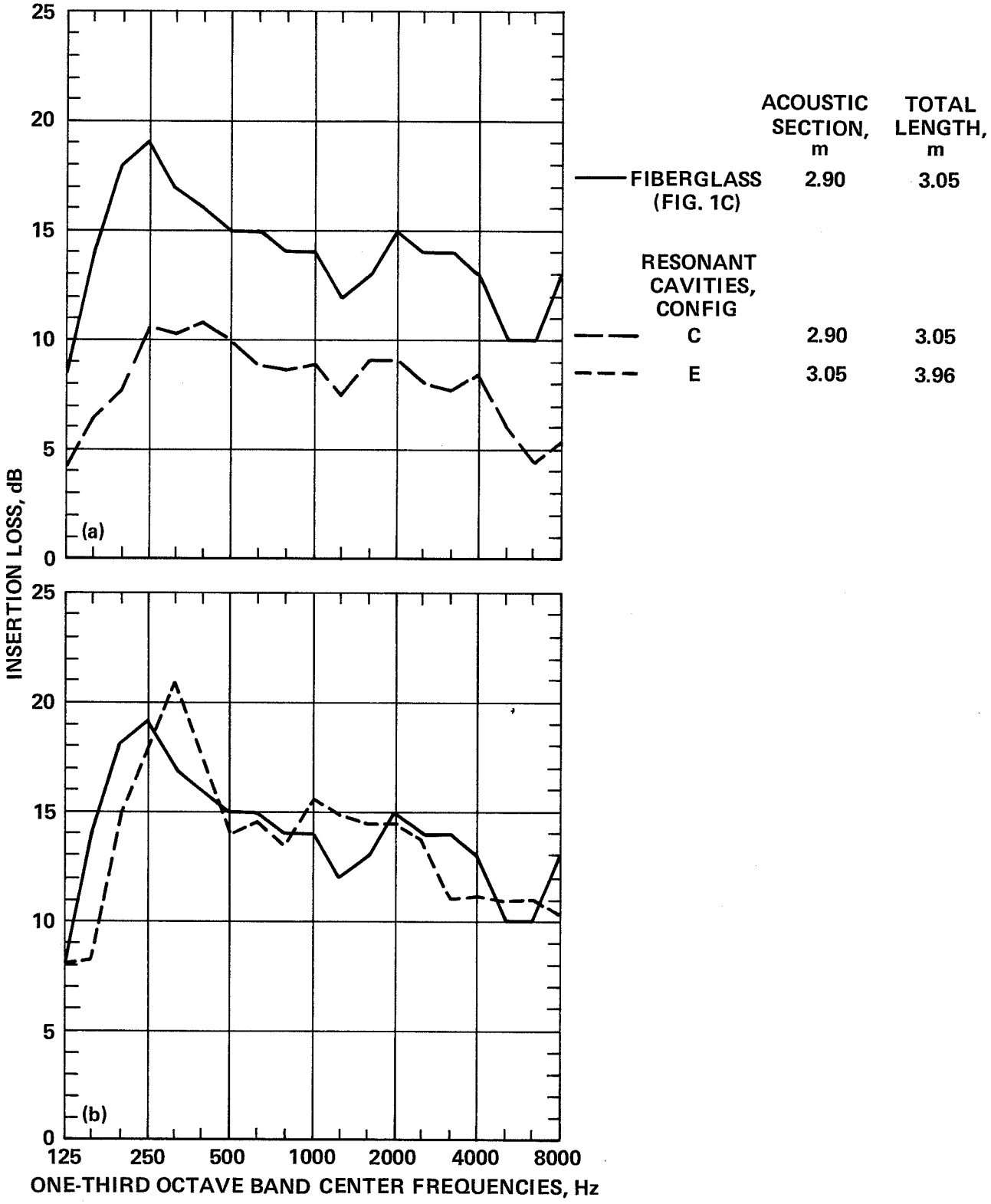

Figure 7.– Comparison of fiberglass silencer and undamped, resonant-cavity silencer: $U = 0$, exhaust simulation. (a) Equal length. (b) Unequal length. Note that configurations E and C have dissimilar cavities and skin.

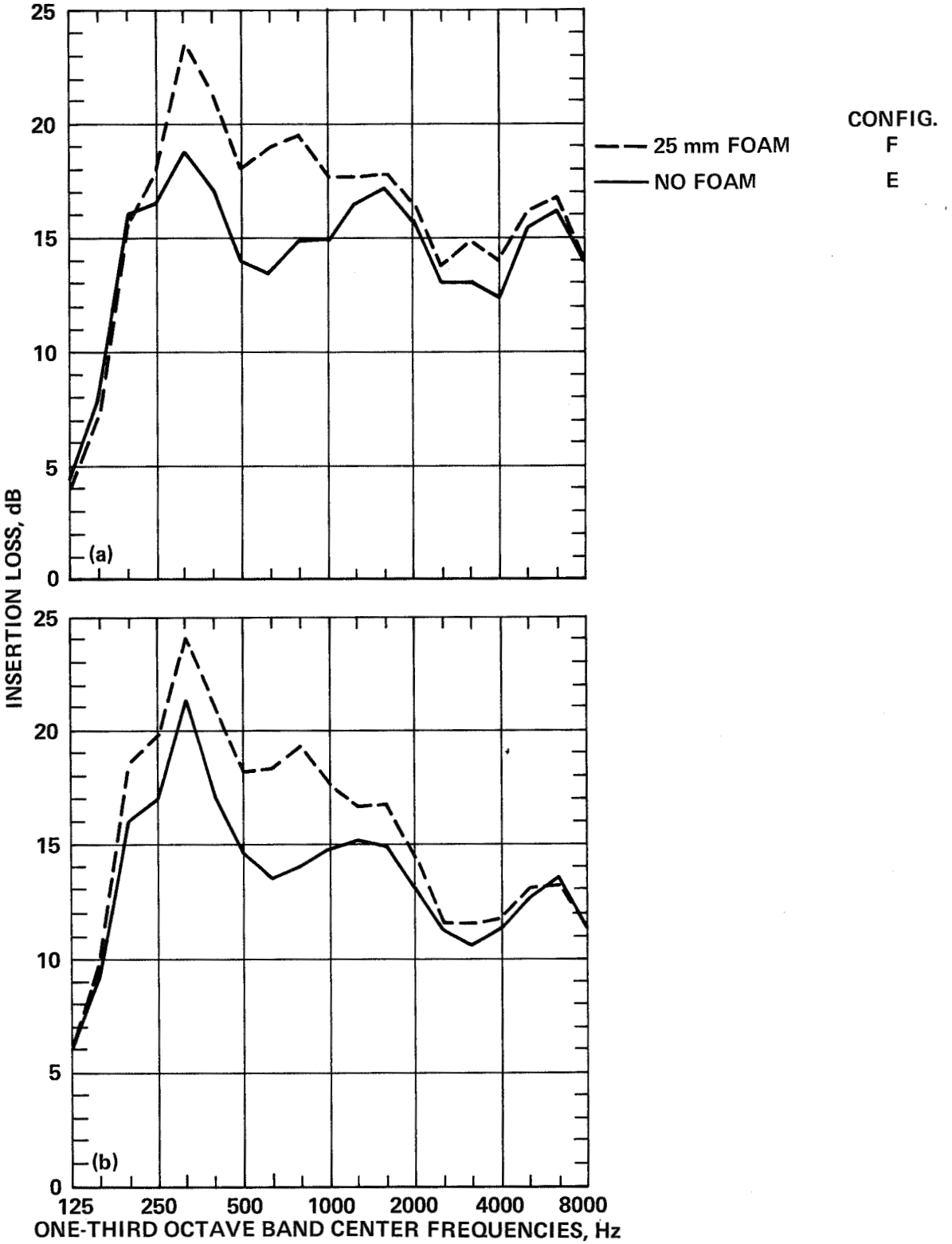

Figure 8.— The effect of foam linings on the cavities' back wall (diagonal septa). (a) $U = 0$, inlet simulation. (b) $U = 17$ m/sec, inlet simulation.

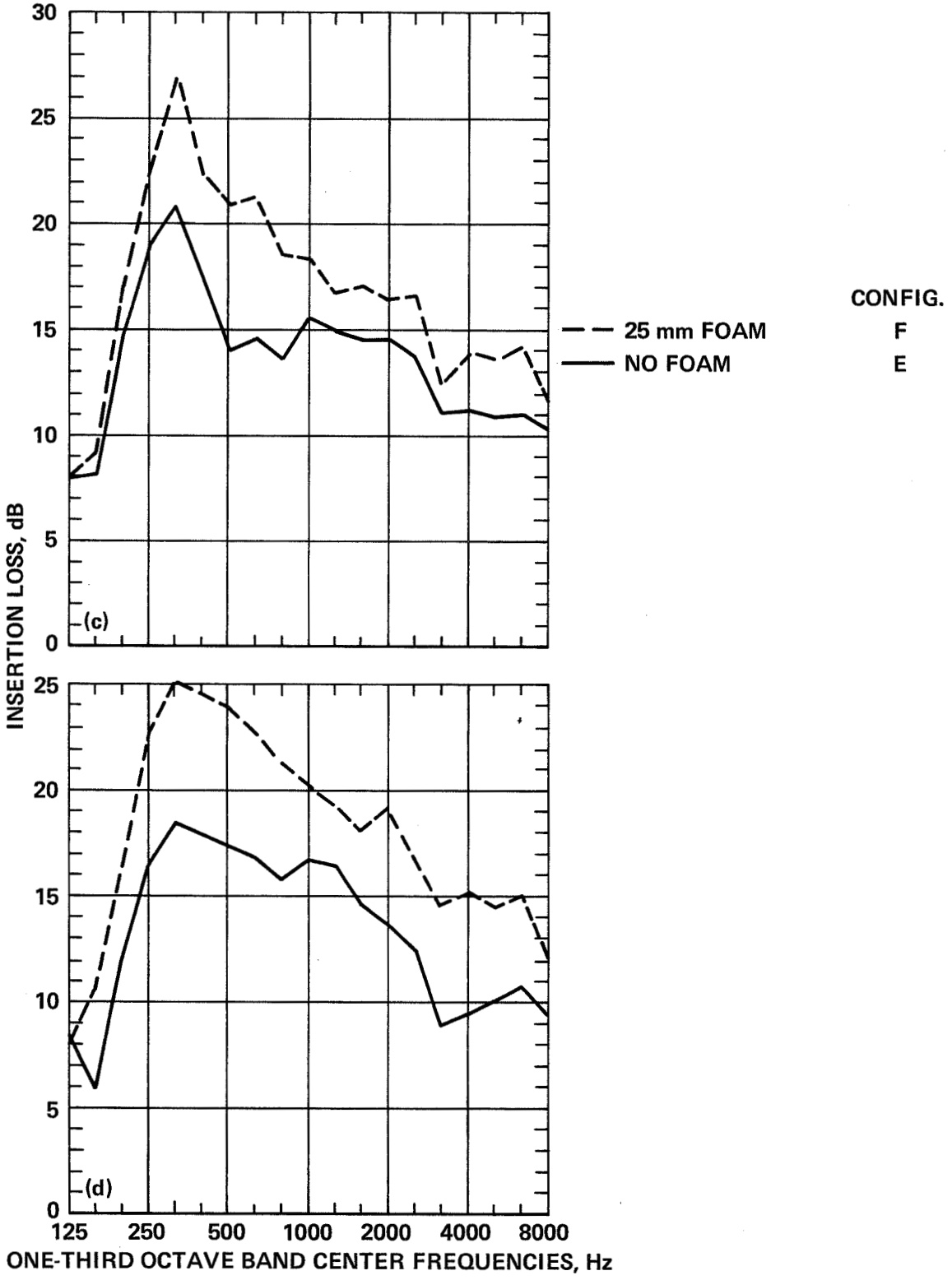

Figure 8.– Concluded. (c) $U = 0$, exhaust simulation. (d) $U = 31$ m/sec, exhaust simulation.

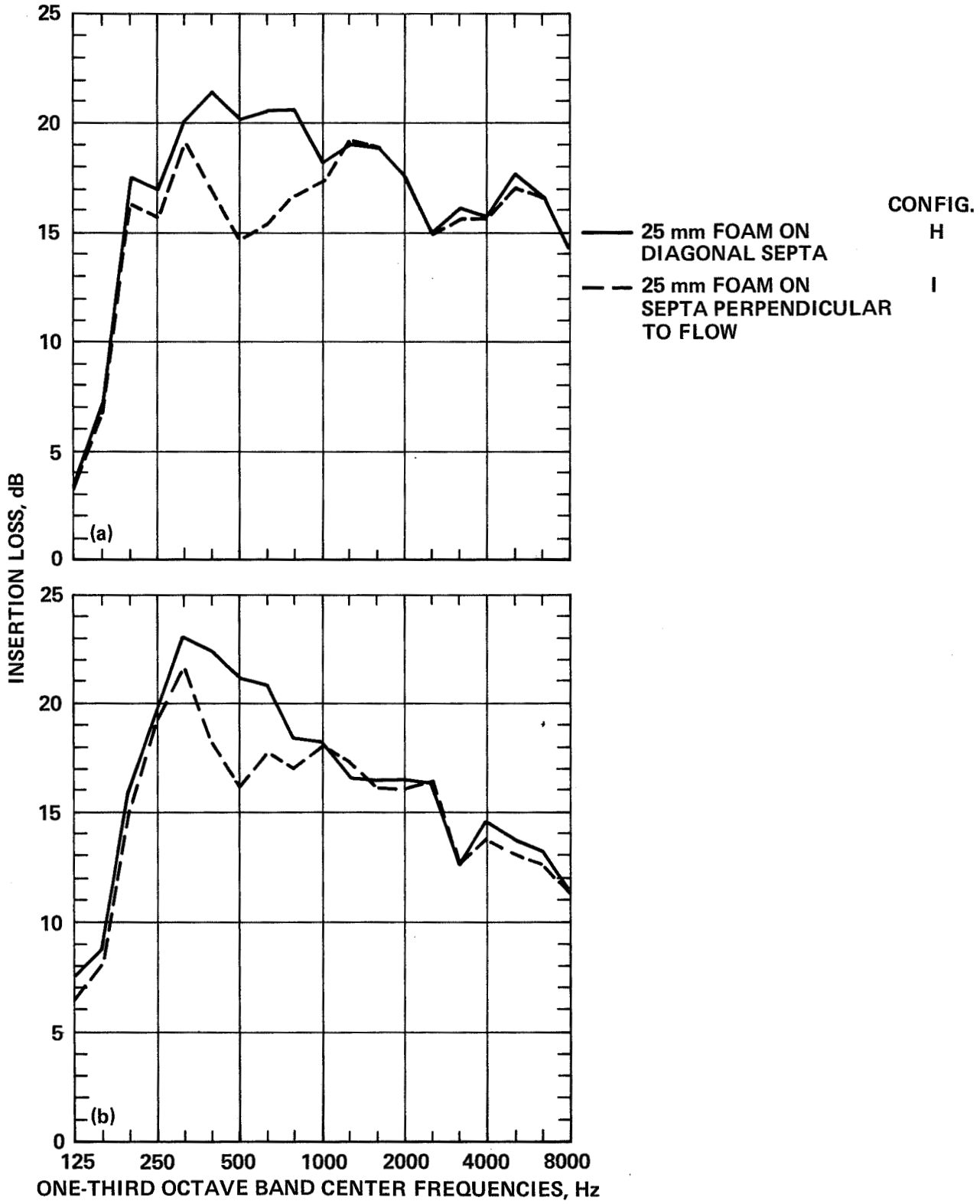

Figure 9.– Effect of cavity lining location on insertion loss.
(a) $U = 0$, inlet simulation. (b) $U = 0$, exhaust simulation.

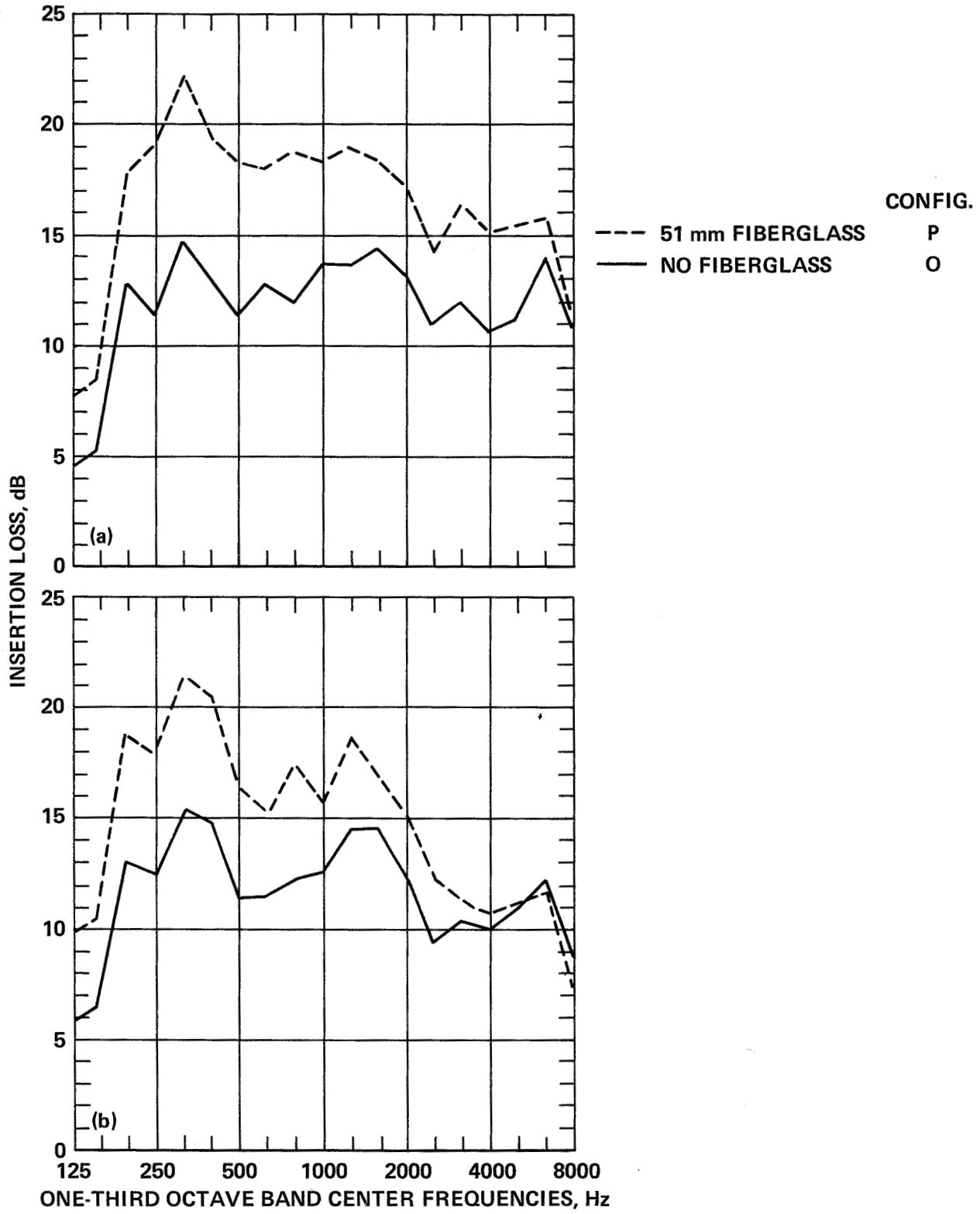

Figure 10.– Effect of fiberglass linings on the cavities' back wall (diagonal septa).
(a) $U = 0$, inlet simulation. (b) $U = 23$ m/sec, inlet simulation.

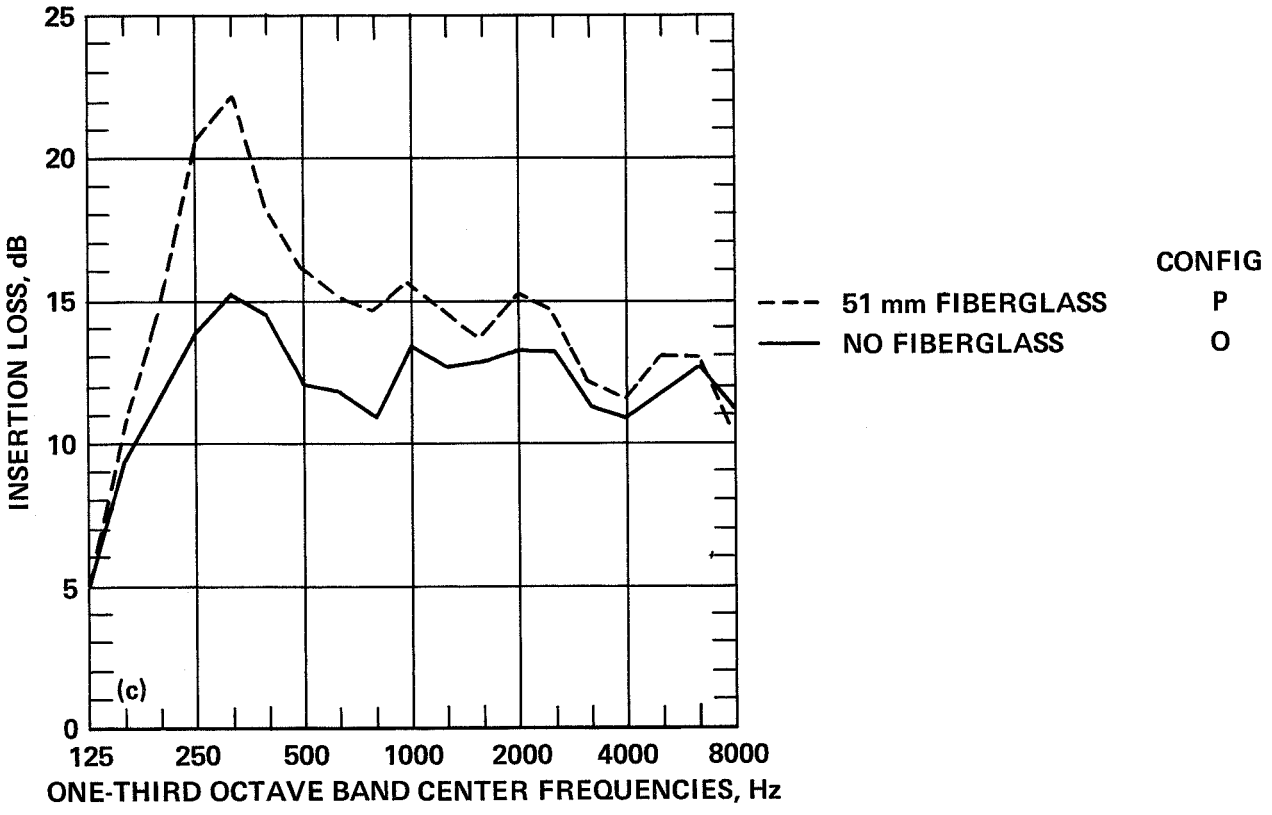

Figure 10.– Concluded. (c) $U = 0$, exhaust simulation.

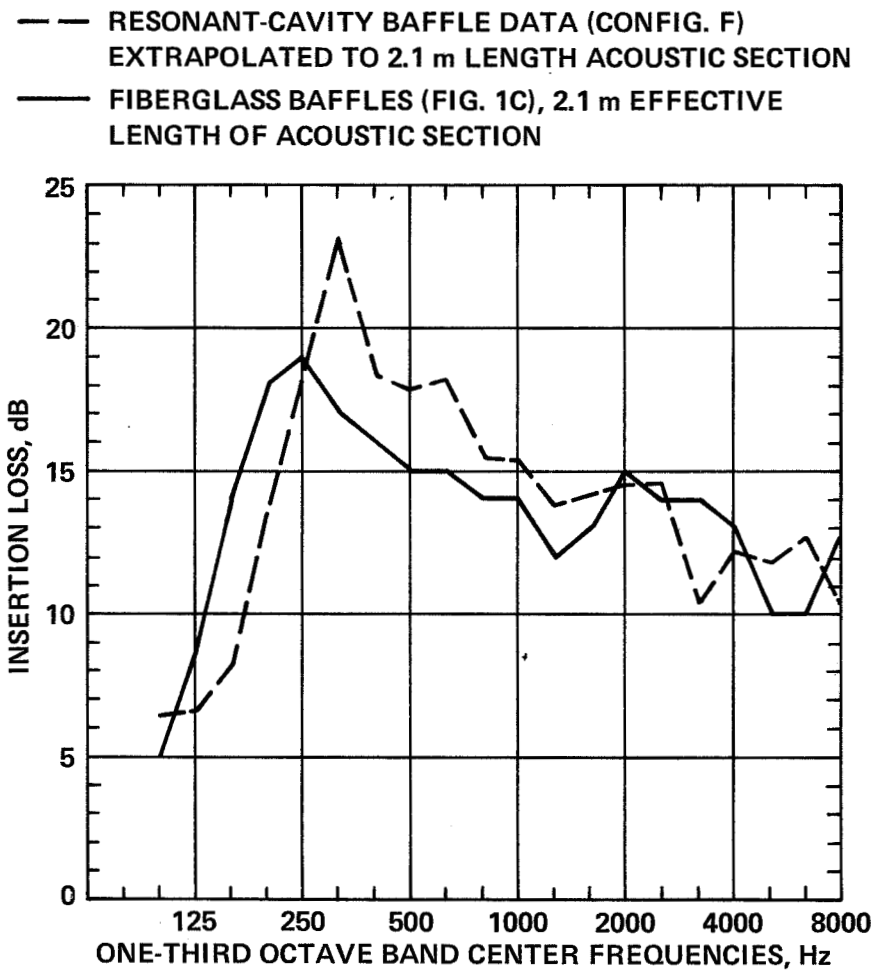

Figure 11.– Comparison of fiberglass silencer and damped, resonant-cavity silencer with equal length acoustic section; the resonant-cavity baffle results were extrapolated from fig. 8(c); $U = 0$, exhaust simulation.

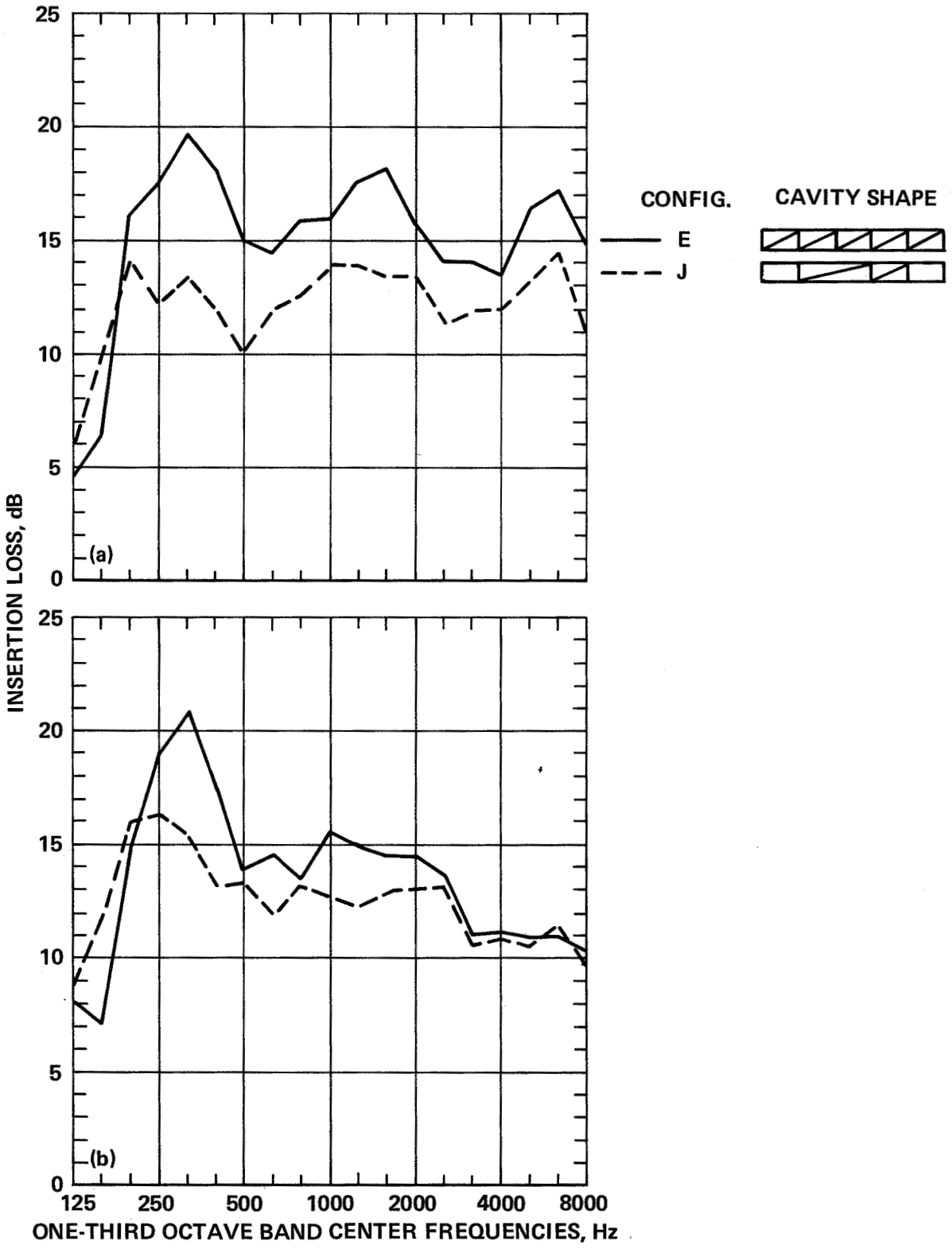

Figure 12.– Effect of cavity geometry on insertion loss. (a) $U = 0$, inlet simulation. (b) $U = 0$, exhaust simulation.

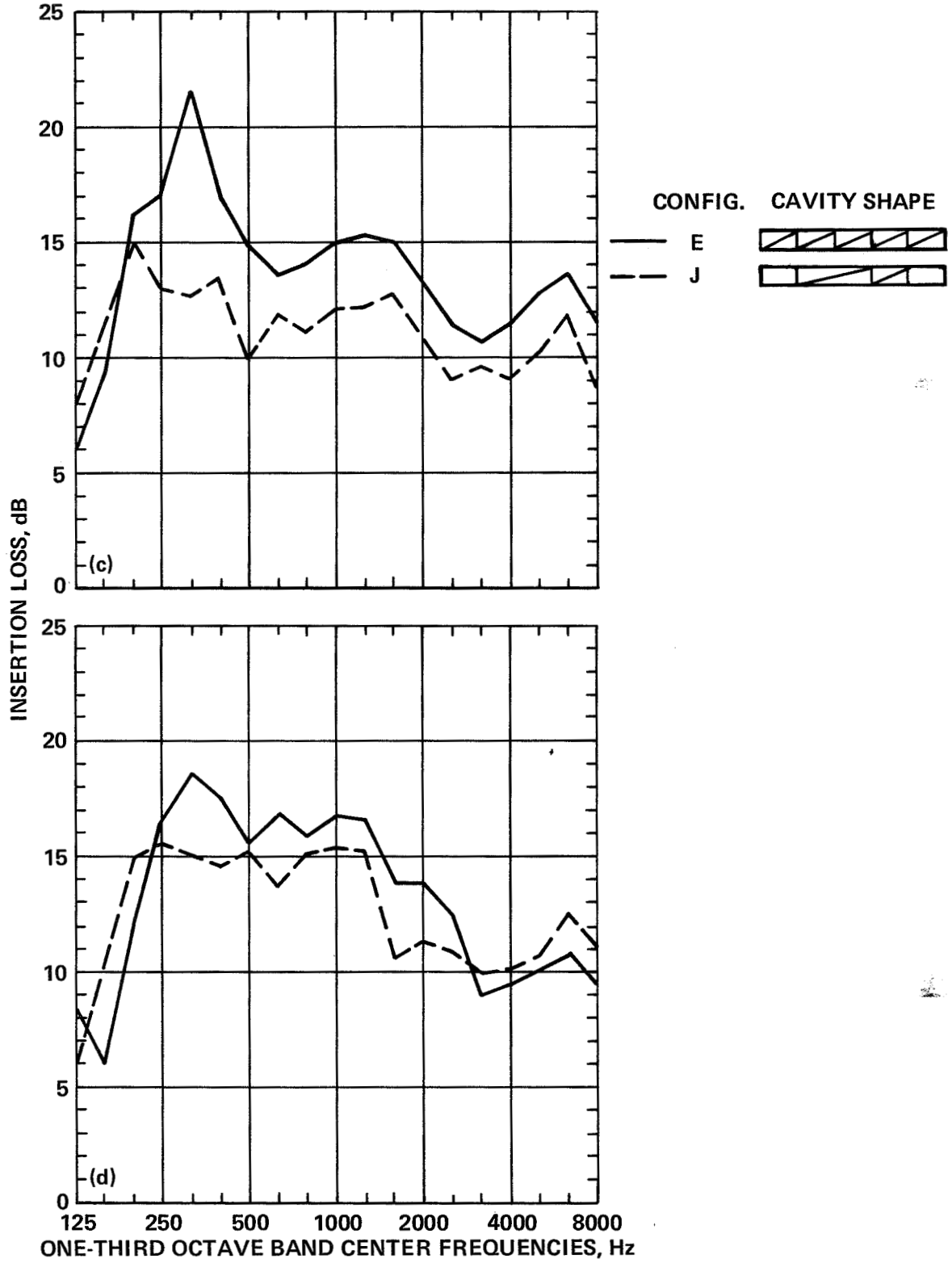

Figure 12.– Concluded. (c) U = 20 m/sec, inlet simulation. (d) U = 31 m/sec, exhaust simulation.

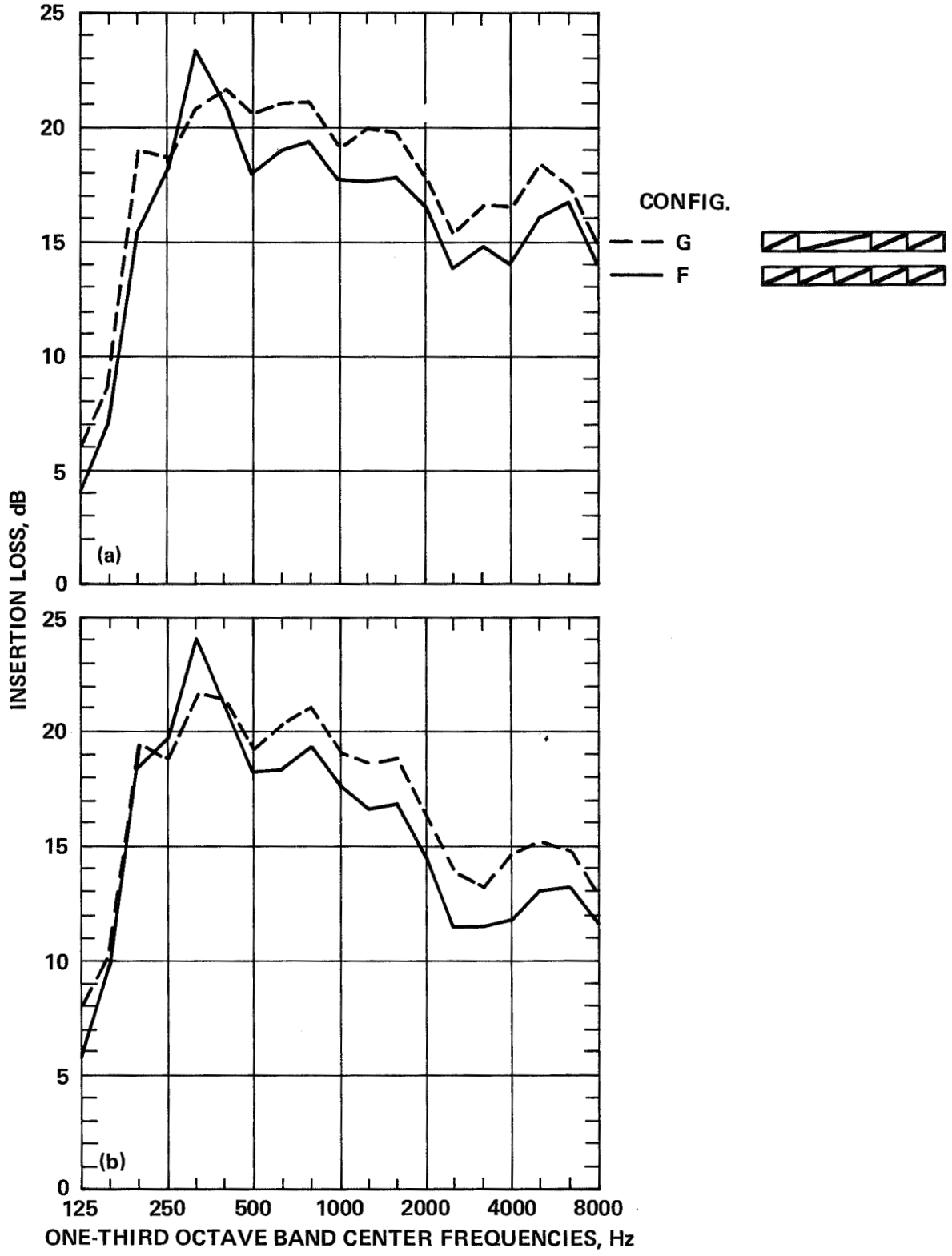

Figure 13.– Comparison of two triangular cavity geometries; both configurations had cavity linings. (a) $U = 0$, inlet simulation. (b) $U = 19$ m/sec, inlet simulation.

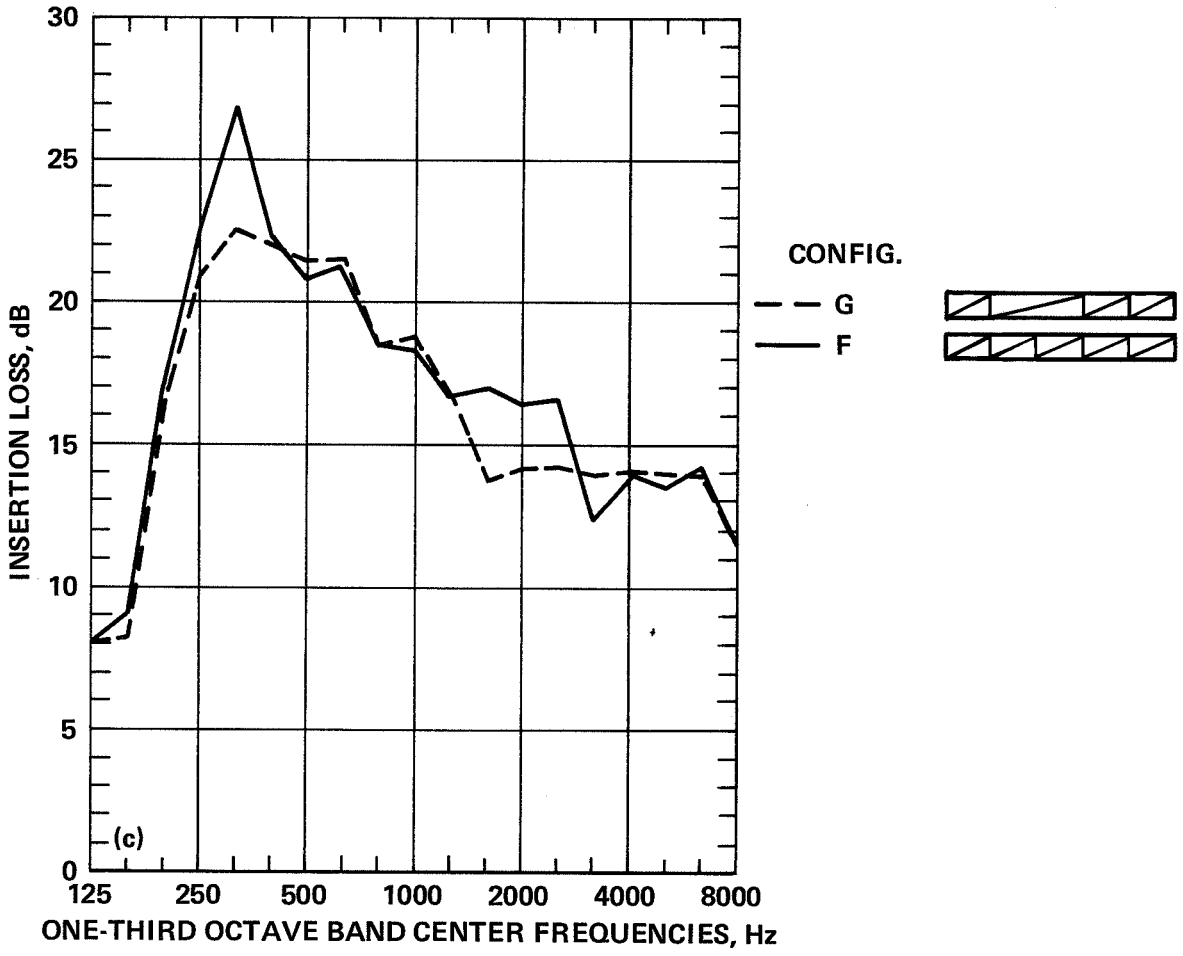

Figure 13.— Concluded. (c) $U = 0$, exhaust simulation.

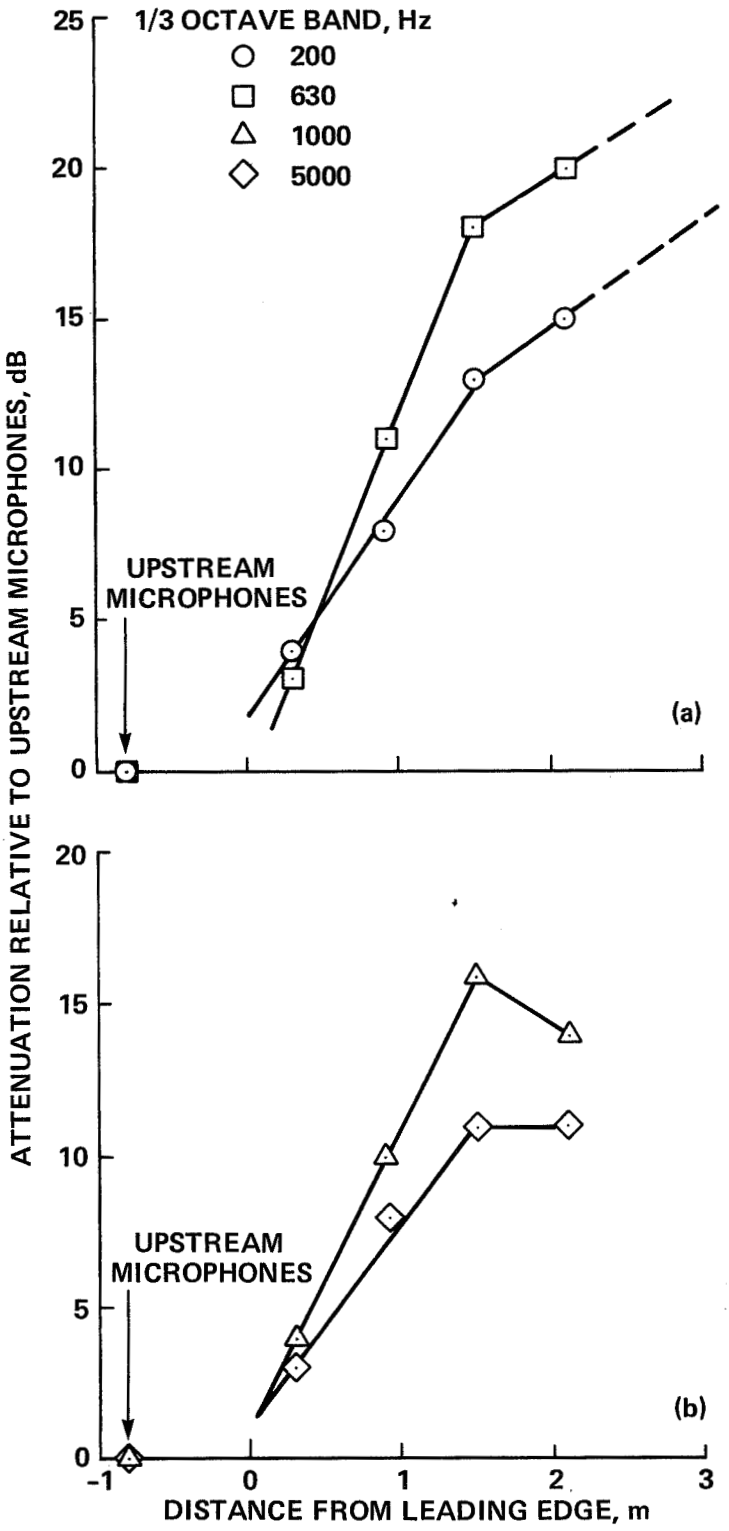

Figure 14.— Acoustic attenuation at several points in fiberglass silencer relative to the four upstream microphones; source streamwise. (a) 200 and 630 Hz third-octave bands. (b) 1000 and 5000 Hz third-octave bands.

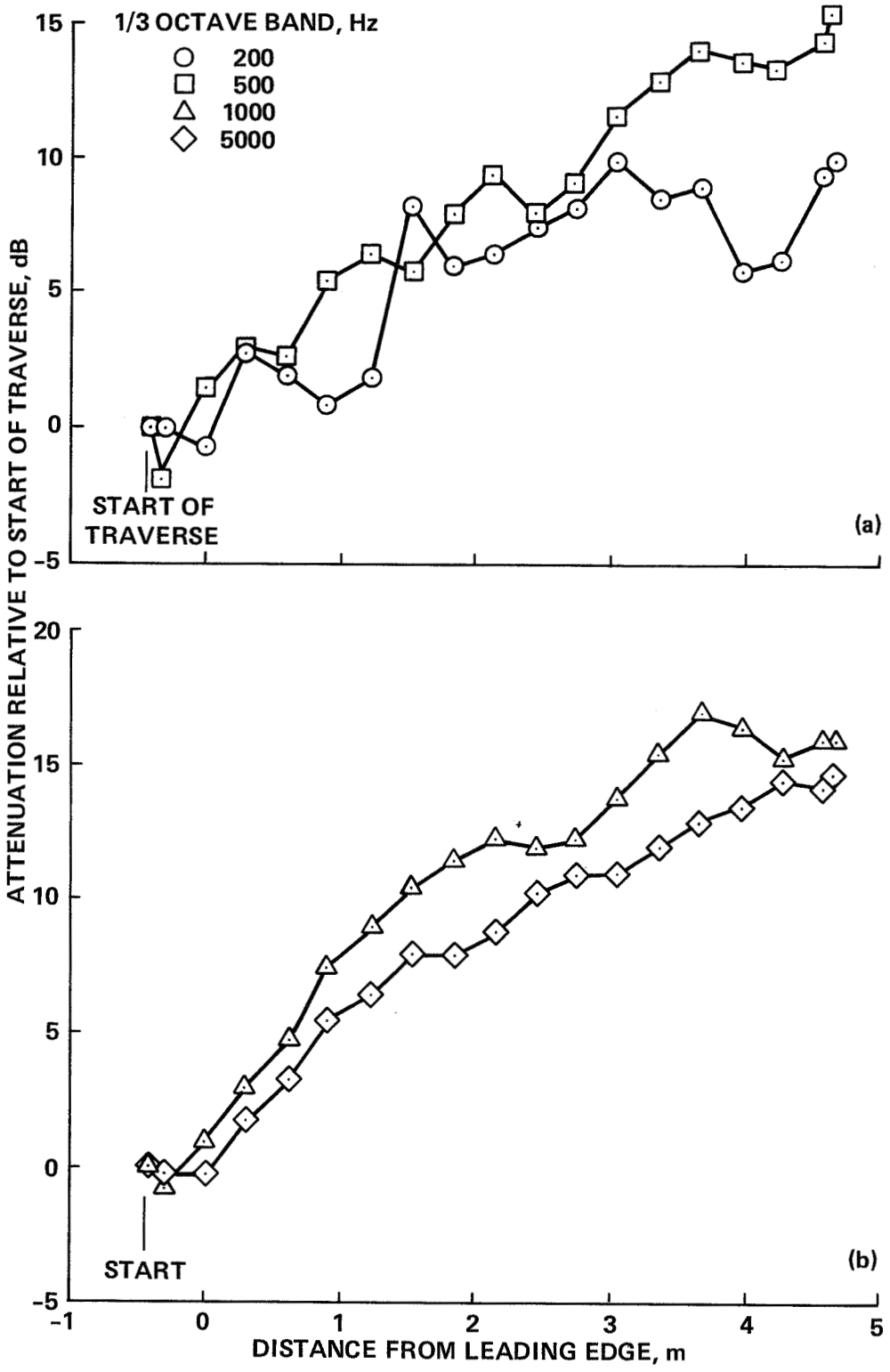

Figure 15.– Acoustic attenuation relative to start of traverse 400 mm upstream of baffle leading edge through resonant-cavity silencer configuration H. (a) Source streamwise, 200 and 500 Hz third-octave bands. (b) Source streamwise, 1000 and 5000 Hz third-octave bands.

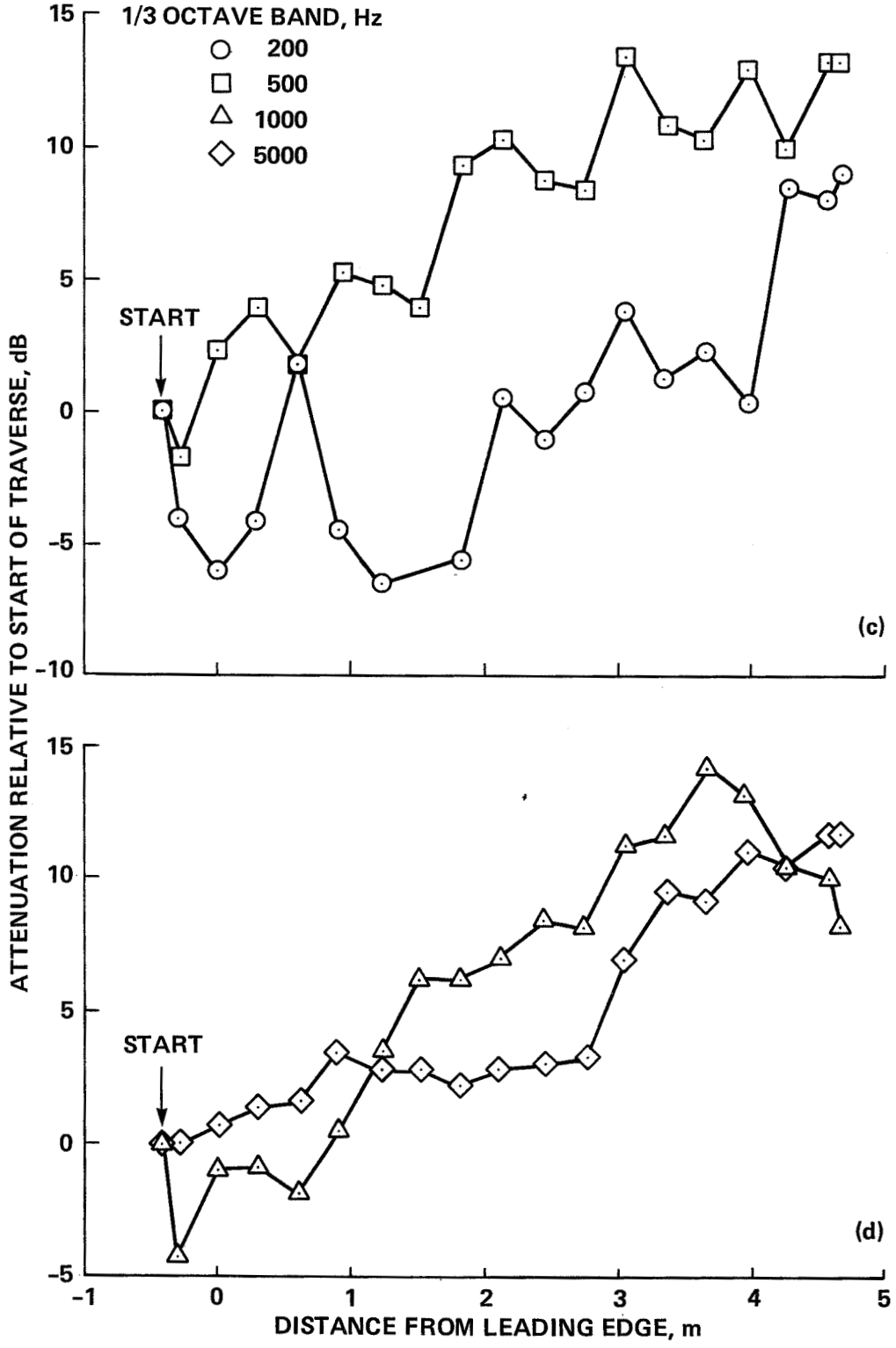

Figure 15.– Concluded. (c) Source 90° to duct, 200 and 500 Hz third-octave bands. (d) Source 90° to duct, 1000 and 5000 Hz third-octave bands.

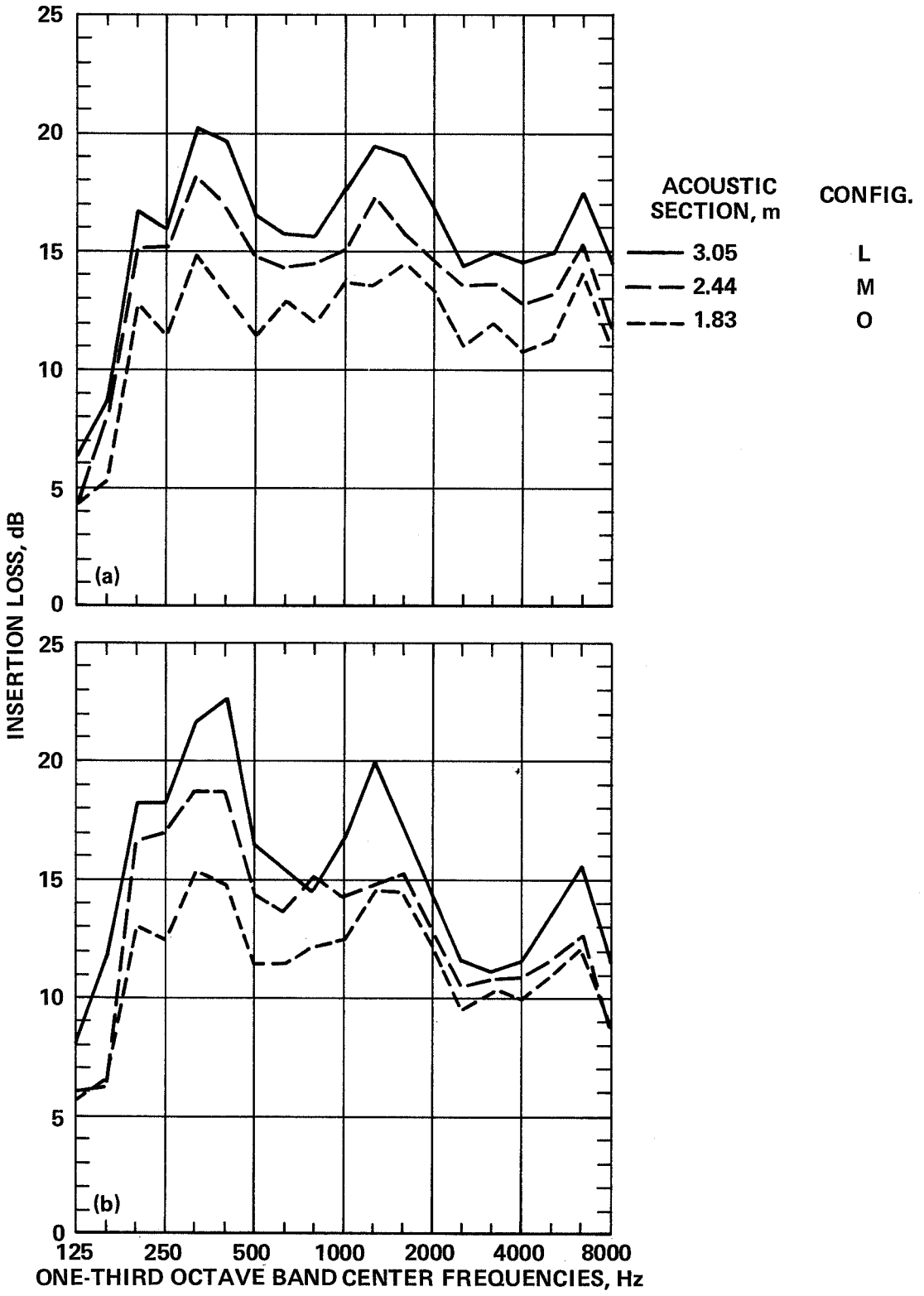

Figure 16.– Comparison of baffles with three different lengths; the constant change in length of 0.61 m is equal to one baffle duct width. (a) $U = 0$, inlet simulation. (b) $U = 23$ m/sec, inlet simulation.

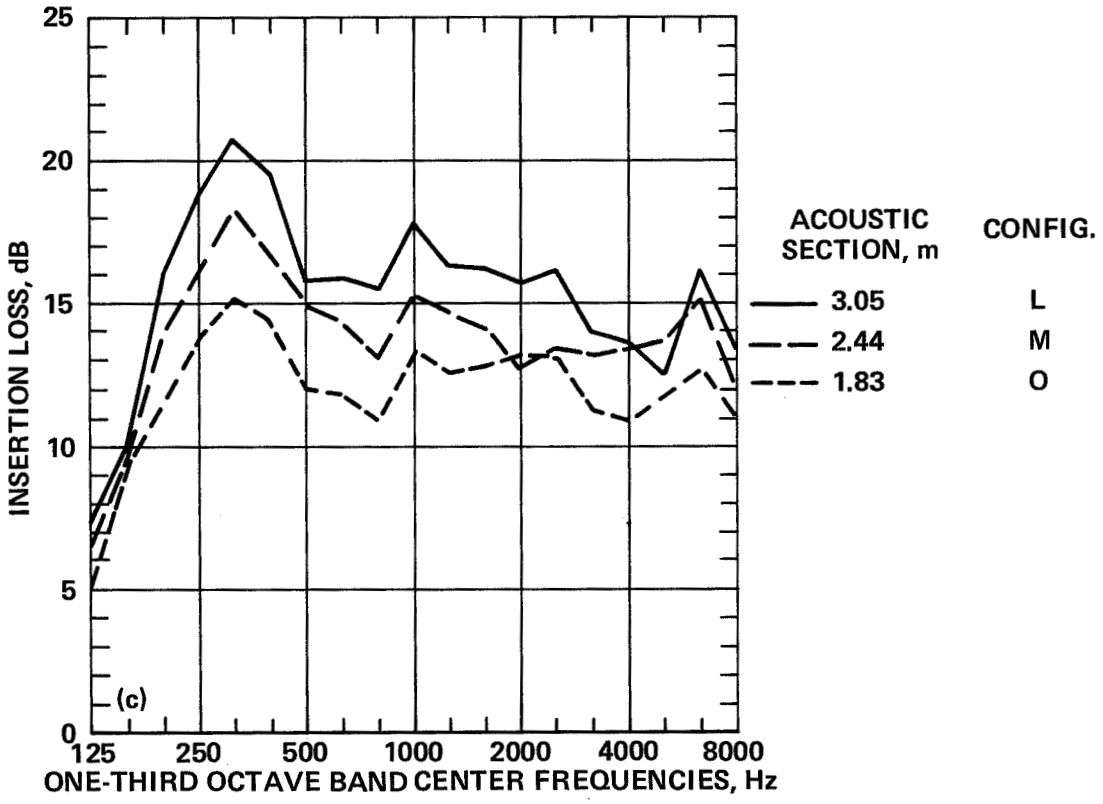

Figure 16.– Concluded. (c) $U = 0$, exhaust simulation.

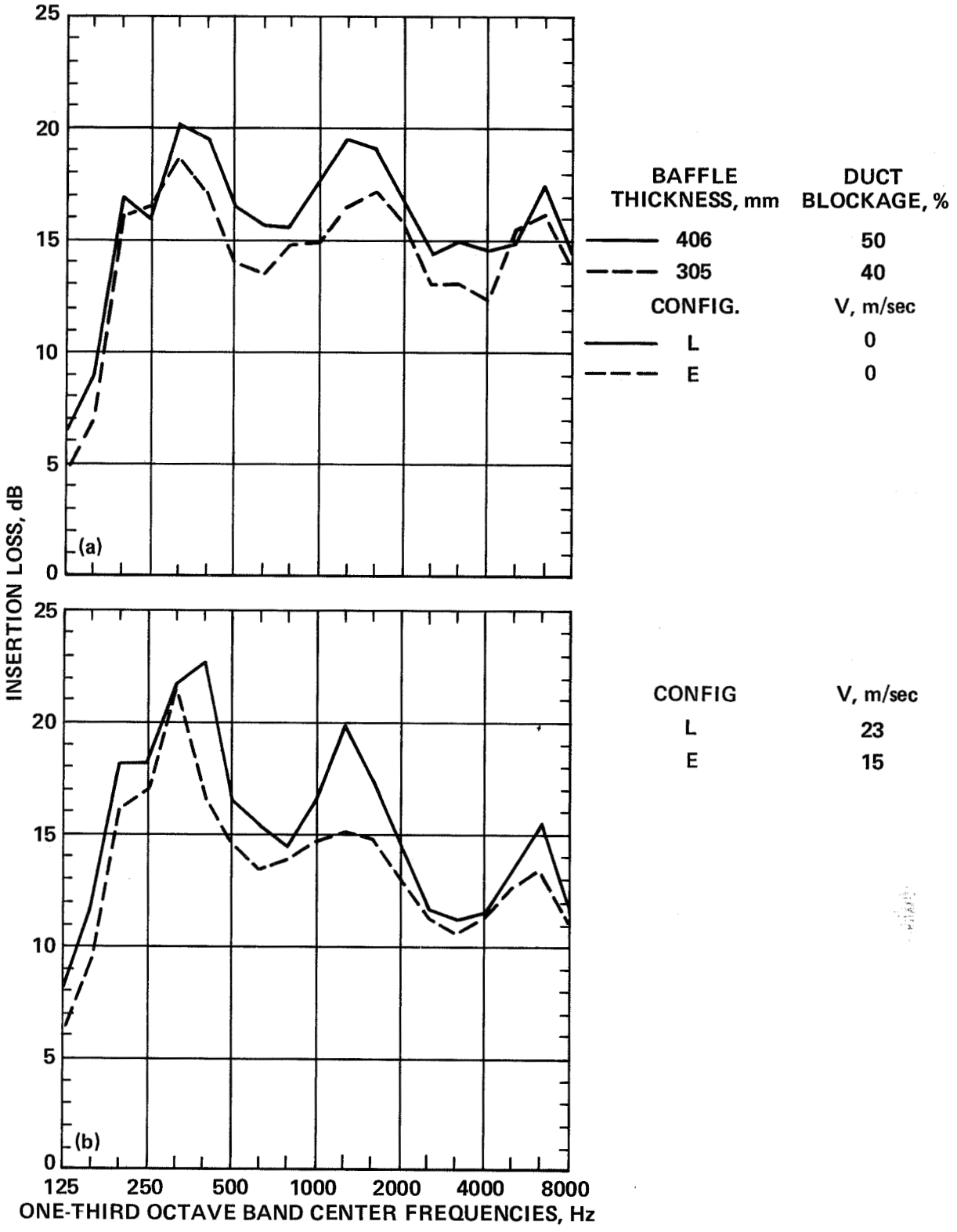

Figure 17.– Effect of baffle thickness and blockage on insertion loss.
(a) $U = 0$, inlet simulation. (b) Inlet simulation.

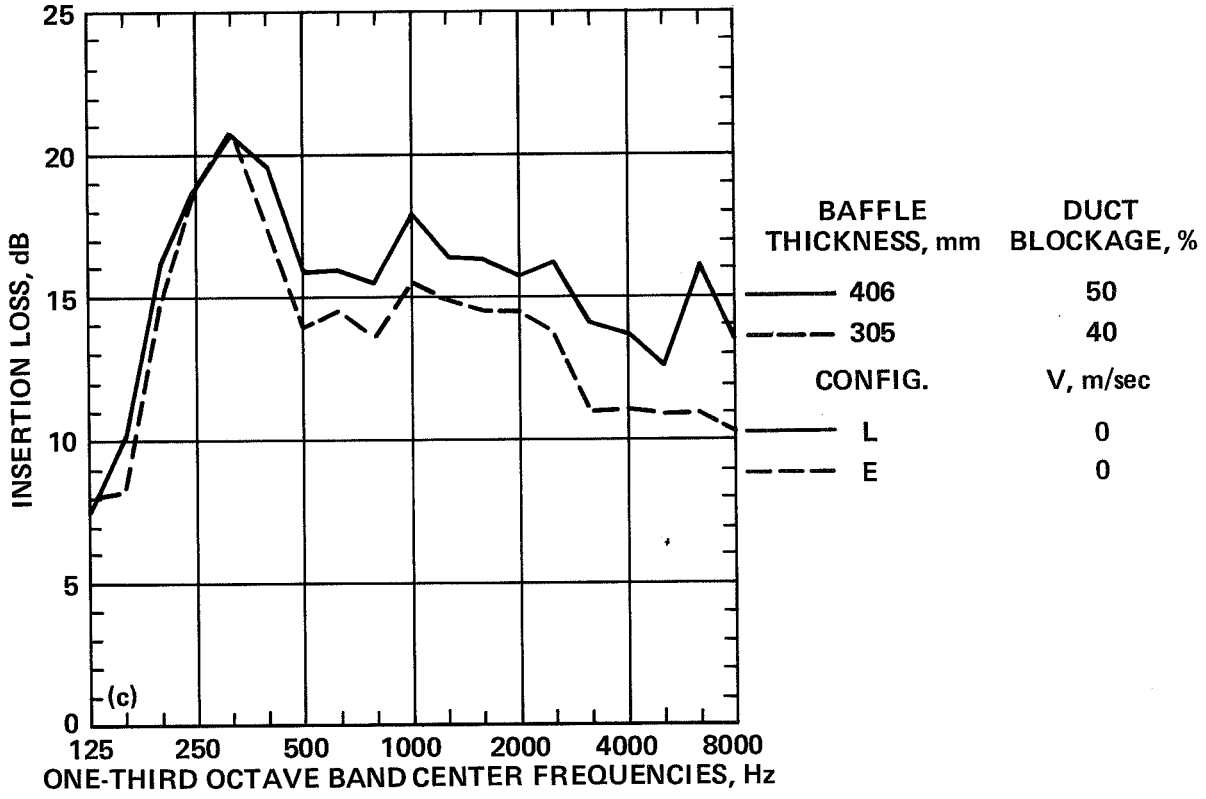

Figure 17.– Concluded. (c) $U = 0$, exhaust simulation.

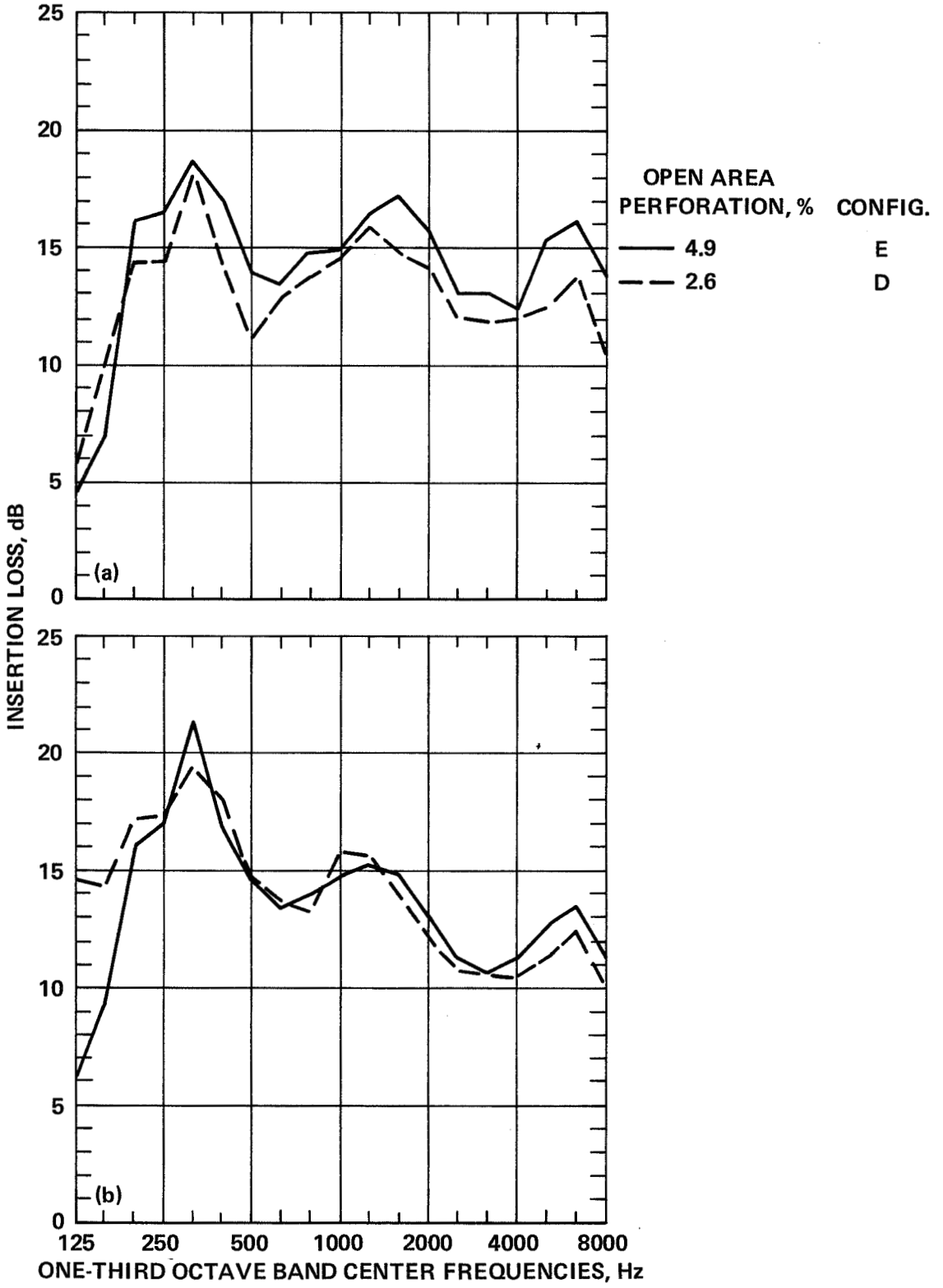

Figure 18.– Effect of skin porosity on insertion loss. (a) $U = 0$, inlet simulation. (b) $U = 19$ m/sec, inlet simulation.

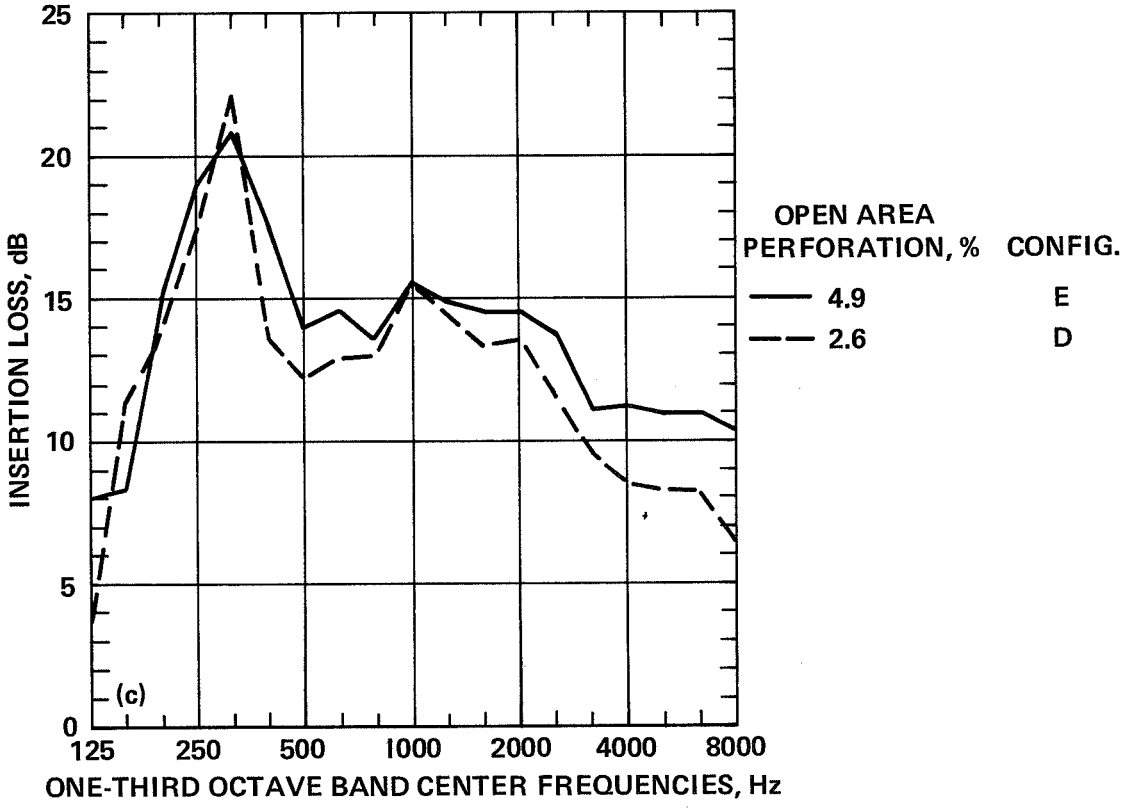

Figure 18.– Concluded. (c) $U = 0$, exhaust simulation.

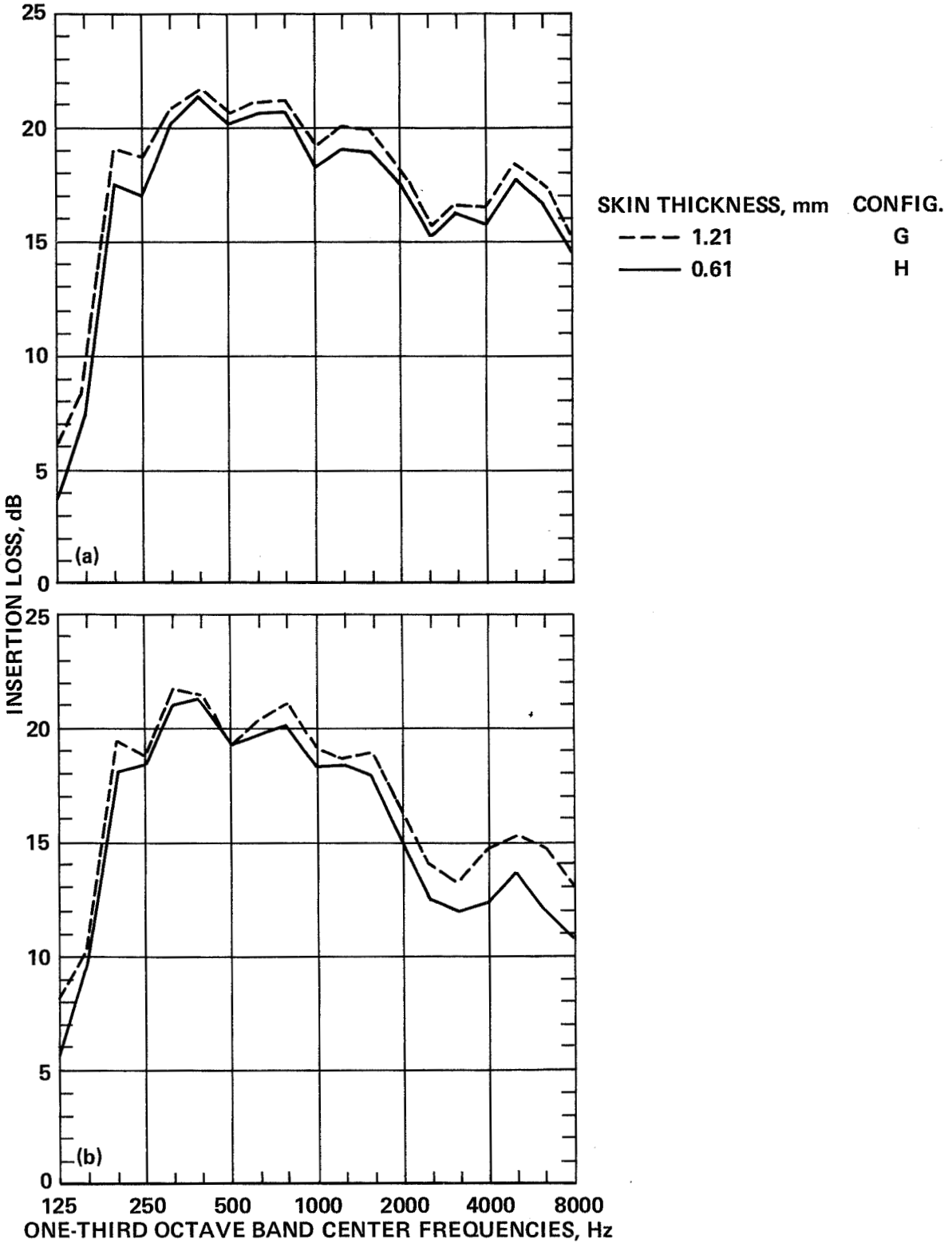

Figure 19.– Effect of skin thickness on insertion loss; the cavities were lined with 25-mm-thick foam, and the open area of the skin was 4.9%. (a) $U = 0$, inlet simulation. (b) $U = 19$ m/sec, inlet simulation.

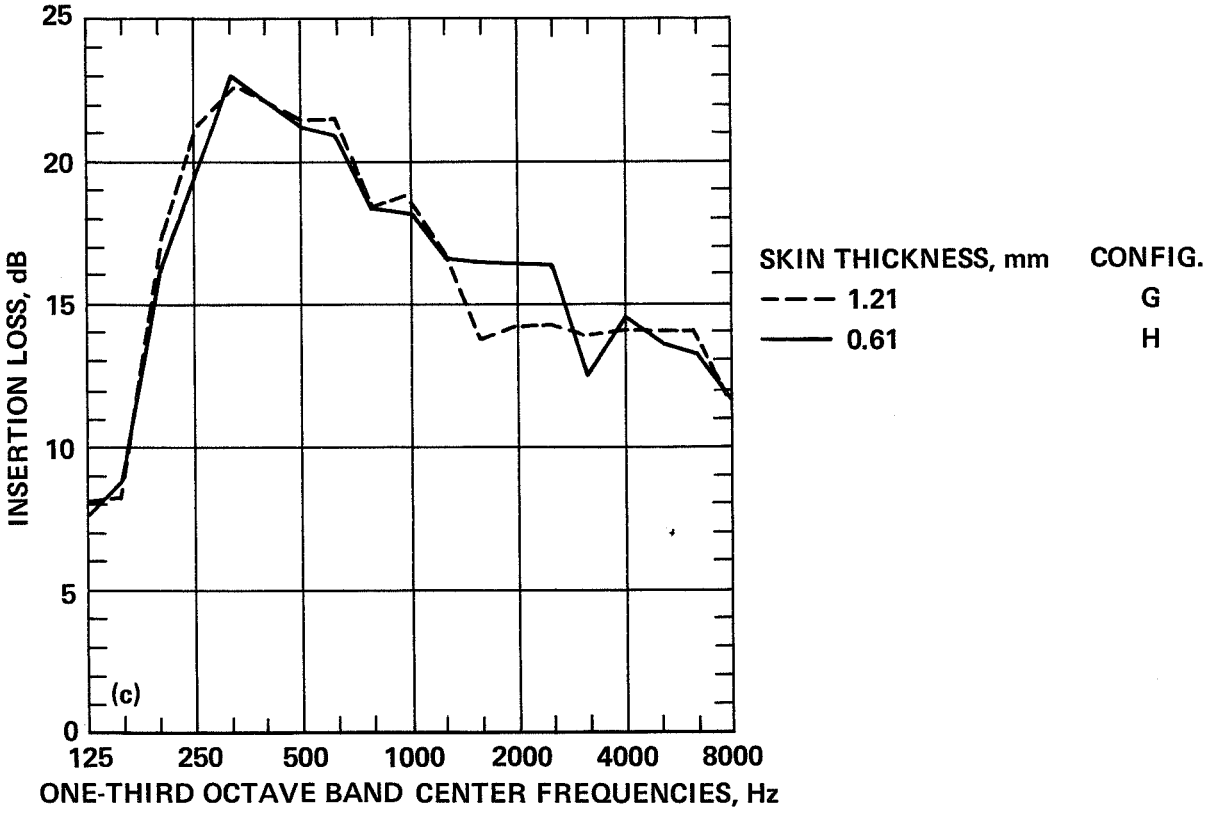

Figure 19.– Concluded. (c) $U = 0$, exhaust simulation.

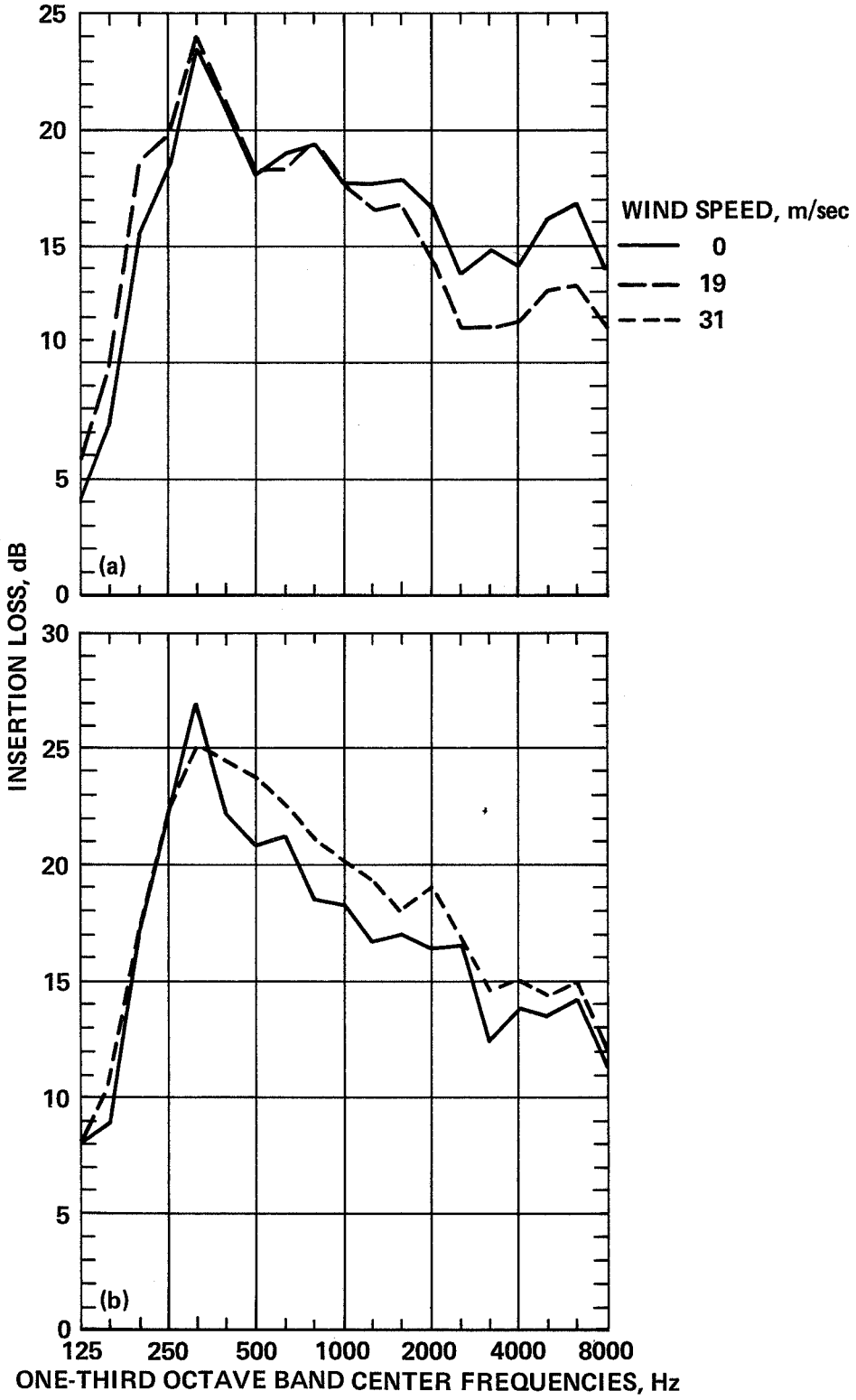

Figure 20.– Effect of wind speed and sound propagation direction on insertion loss: configuration F. (a) Inlet simulation (upstream sound propagation). (b) Exhaust simulation (downstream sound propagation).

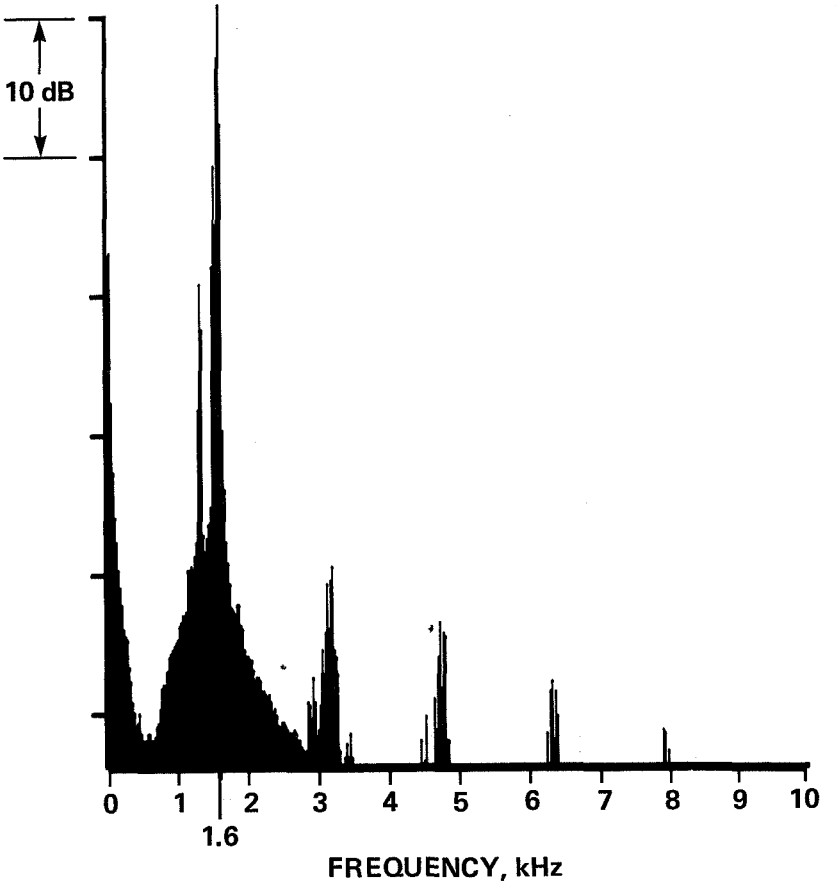

(a) $U = 23$ m/sec.

Figure 21.– Flow-induced cavity tones from configuration N, an unlined baffle configuration. Filter bandwidth = 25 Hz.

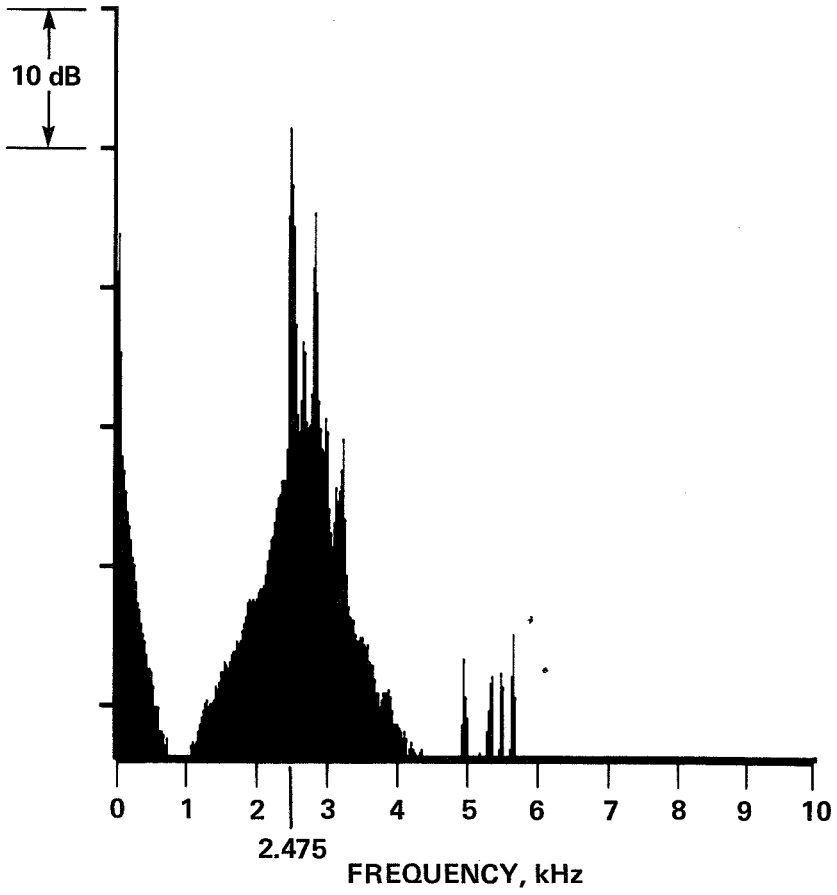

(b) $U = 37$ m/sec.

Figure 21.– Continued.

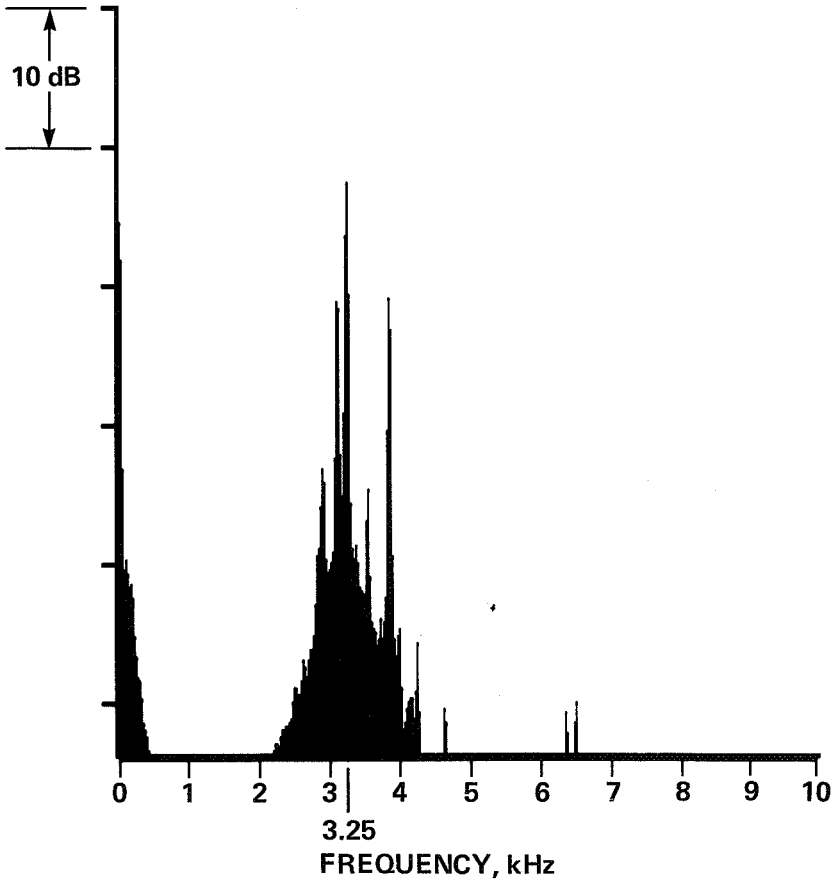

(c) $U = 44$ m/sec.

Figure 21.– Concluded.

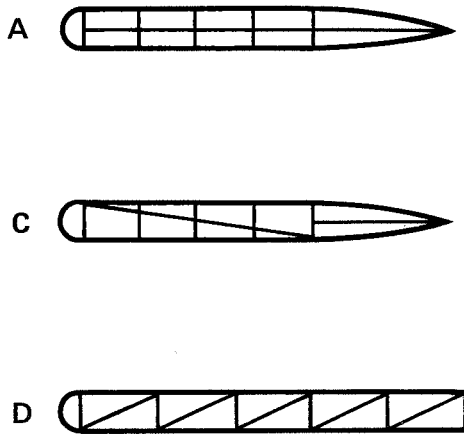

U^*	$f_t^\dagger$	f_s^{**}	
22.3 m/sec	2500 Hz	2537 Hz	(1/3 OCT. BAND)
28.3	3150^+	3219	
37.7	5000^-	4288	
43.6	5000	4960	
35.8	—	4072	(AUDIBLE BUT
48.4	—	5506	NOT RECORDED)
40.6	4275-5400	4618	MULTIPLE TONES
54.1	5400-7700	6154	

*U = SPEED AT WHICH FIRST TONE WAS AUDIBLE AND SUBSEQUENT SPEEDS AT WHICH TONE SHIFTED FREQUENCY

$^\dagger f_t$ = MEASURED TONAL FREQUENCY

$^{**} f_s$ = CALCULATED VORTEX SHEDDING FREQUENCY FROM EQUATIONS 14 AND 15

Figure 22.– Flow-induced cavity tones from several configurations and wind speeds; 2.6% skin porosity.

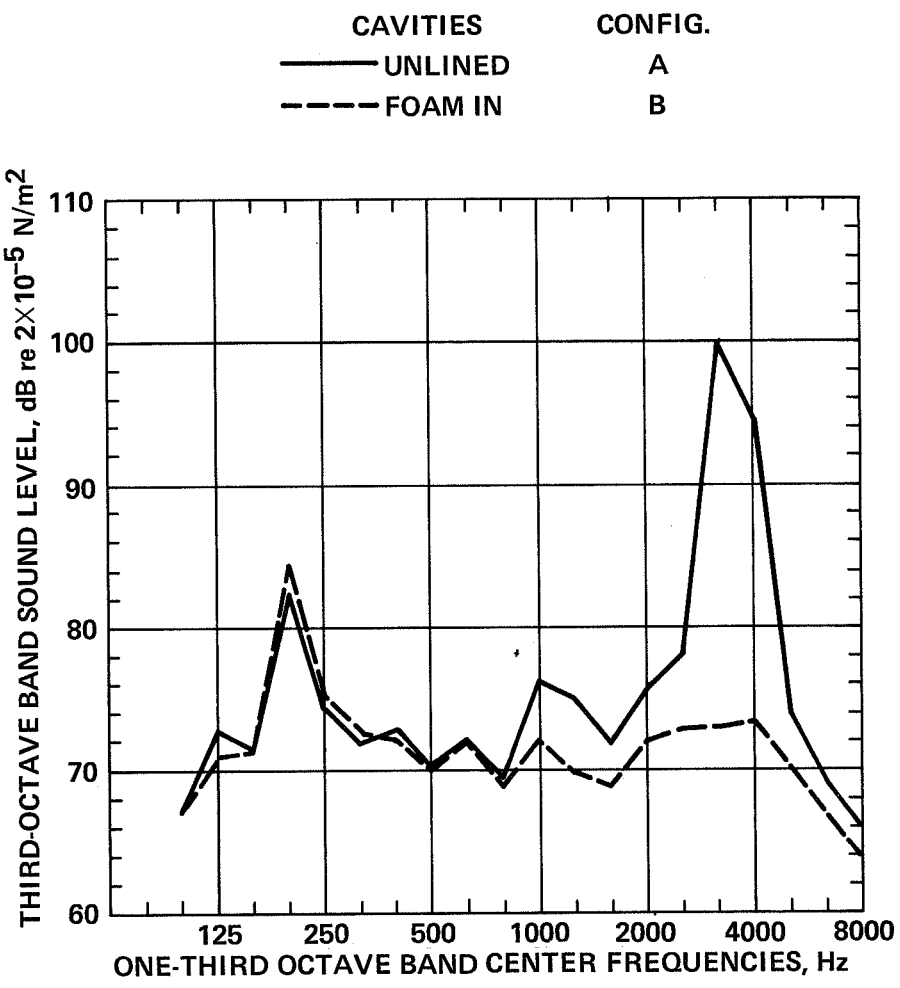

Figure 23.– Effect of cavity damping on tones: $U = 28$ m/sec.

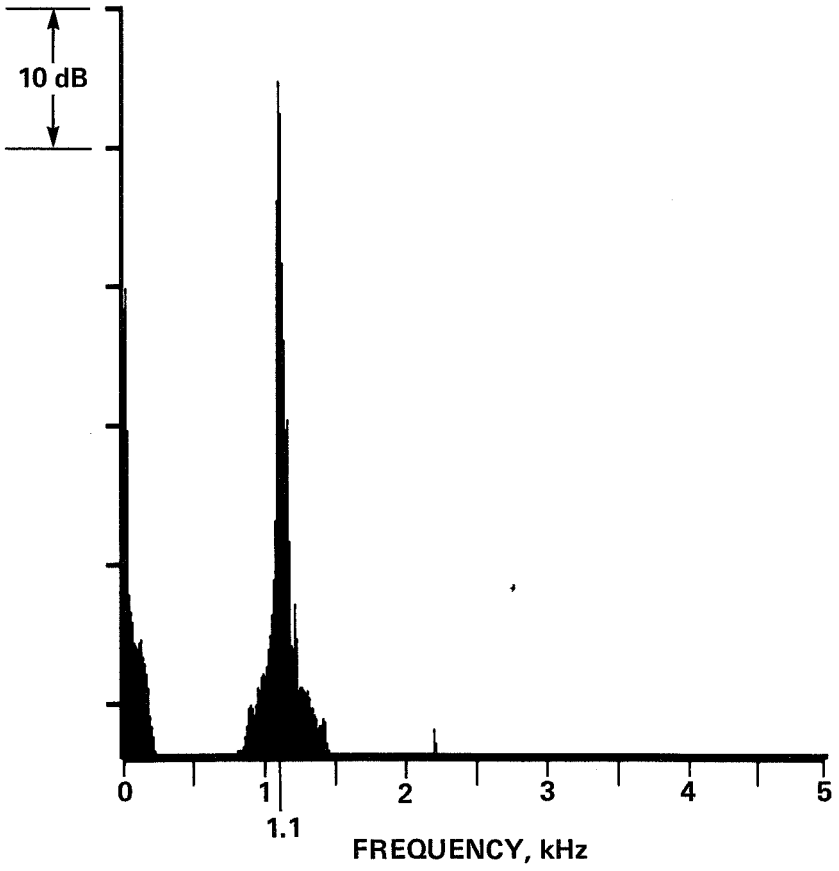

Figure 24.– Duct resonances due to configuration K: U = 22 m/sec; filter bandwidth = 12.5 Hz.

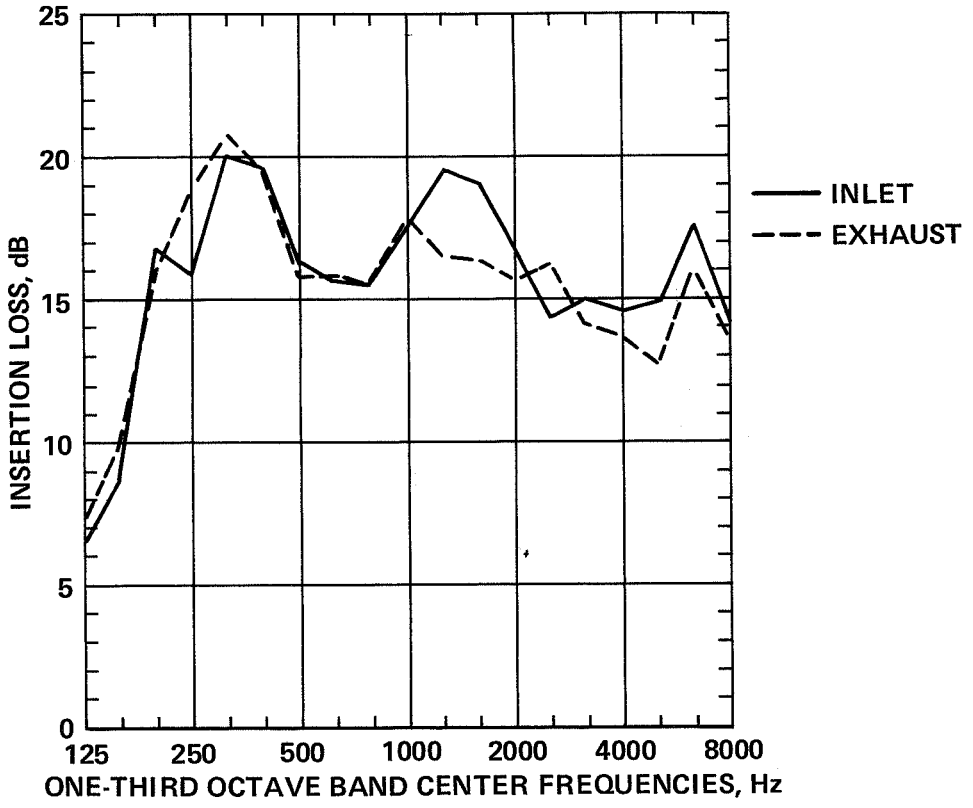

Figure 25.– Comparison of inlet and exhaust silencer performance: configuration L, $U = 0$.

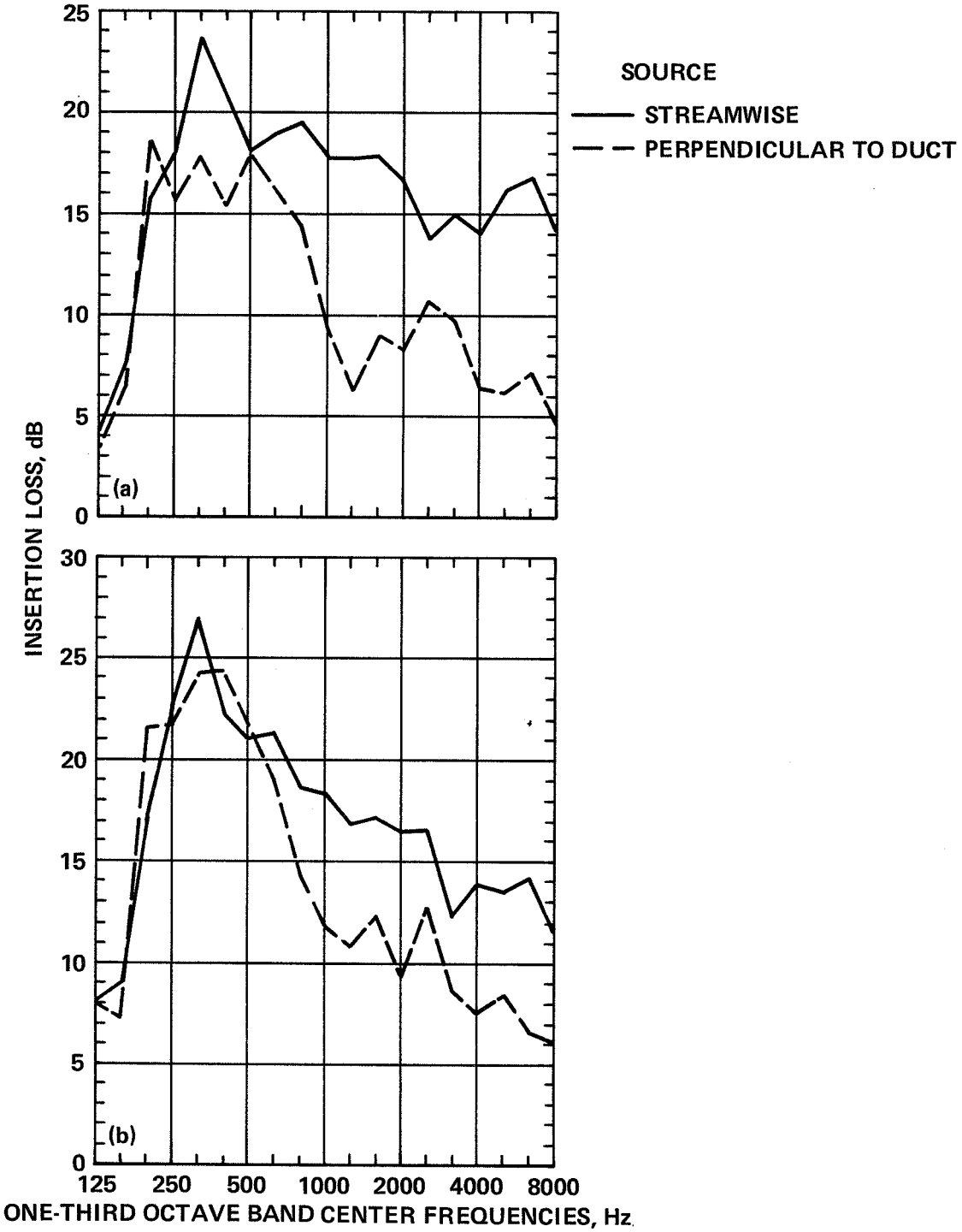

Figure 26.– Effect of acoustic source orientation on insertion loss: configuration F, $U = 0$.
(a) Inlet simulation. (b) Exhaust simulation.

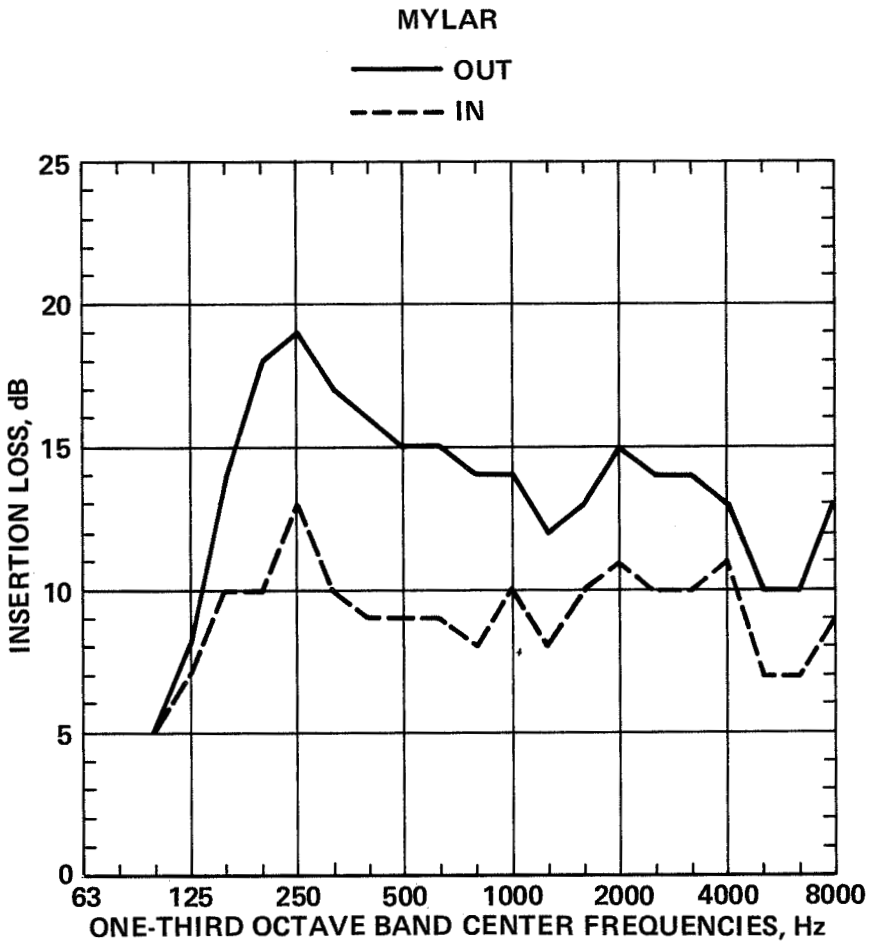

Figure 27.– Effect of fiberglass-silencer performance of a Mylar membrane installed between the fiberglass and perforated skin.

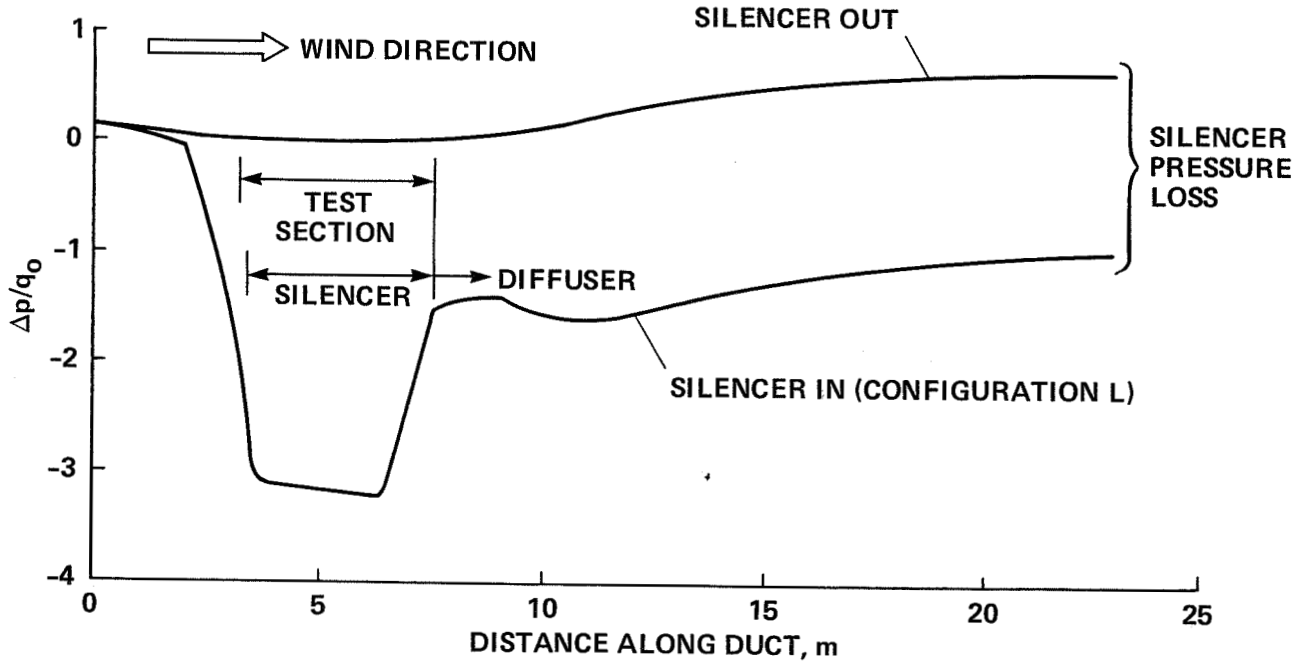

Figure 28.– Typical static pressure change along the duct normalized by free-stream dynamic pressure, with and without silencer installed: U_O = 24 m/sec.

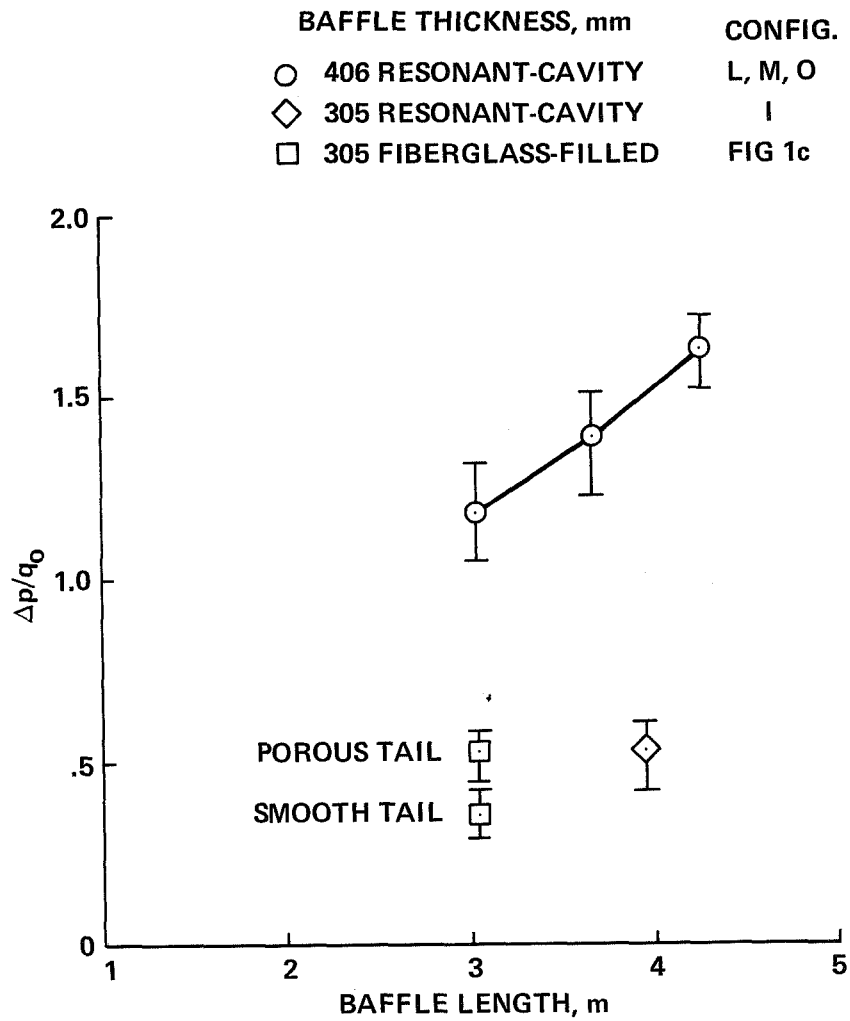

Figure 29.– The static or total pressure loss through the silencer normalized by free-stream dynamic pressure: U_o = 24 m/sec.

1. Report No. NASA TP-1970 AVRADCOM TR 81-A-2	2. Government Accession No.	3. Recipient's Catalog No.
4. Title and Subtitle A STUDY OF RESONANT-CAVITY AND FIBERGLASS-FILLED PARALLEL BAFFLES AS DUCT SILENCERS		5. Report Date April 1982 6. Performing Organization Code
7. Author(s) Paul T. Soderman		8. Performing Organization Report No. A-8363 10. Work Unit No. 505-31-21
9. Performing Organization Name and Address Ames Research Center and Aeromechanics Laboratory AVRADCOM Research and Technology Laboratories Moffett Field, Calif. 94035		11. Contract or Grant No. 13. Type of Report and Period Covered Technical Paper
12. Sponsoring Agency Name and Address National Aeronautics and Space Administration, Washington, D. C. 20546, and U.S. Army Aviation Research and Development Command, St. Louis, Mo. 63166		14. Sponsoring Agency Code

15. Supplementary Notes

Point of contact: Paul T. Soderman, Ames Research Center, 247-1, Moffett Field, CA, (415)965-6675 or FTS 448-6675.

16. Abstract

Acoustical performance and pressure drop were measured for two types of splitters designed to attenuate sound propagating in ducts – resonant-cavity baffles and fiberglass-filled baffles. Arrays of four baffles were evaluated in the 7- by 10-Foot Wind Tunnel Number 1 at Ames Research Center at flow speeds from 0 to 41 m/sec. The baffles were 2.1 m high, 305 to 406 mm thick, and 3.1 to 4.4 m long. Emphasis was on measurements of silencer insertion loss as affected by variations of such parameters as baffle length, baffle thickness, perforated skin geometry, cavity size and shape, cavity damping, wind speed, and acoustic field directivity. An analytical method for predicting silencer performance is described and compared with measurements.

Unlike small, single-orifice resonators, the undamped, resonant-cavity baffles attenuated sound over a broad frequency range. With the addition of cavity damping in the form of 25-mm foam linings, the insertion loss above 250 Hz of the resonant-cavity baffles was improved 2 to 7 dB compared with the undamped baffles; the loss became equal to or greater than the insertion loss of comparable size fiberglass baffles at frequencies above 250 Hz. Variations of cavity size and shape showed that a series of cavities with triangular cross-sections (i.e., variable depth) were superior to cavities with rectangular cross sections (i.e., constant depth). In wind, the undamped, resonant-cavity baffles generated loud cavity-resonance tones; the tones could be eliminated by cavity damping. Duct-resonance tones were also generated by configurations that had solid skin over portions of the baffle surfaces. The effects of skin porosity, baffle length, and baffle thickness are documented.

17. Key Words (Suggested by Author(s))	18. Distribution Statement
Silencer Duct acoustics Acoustic baffles Acoustic resonators	Unclassified - Unlimited Subject Category 71

19. Security Classif. (of this report)	20. Security Classif. (of this page)	21. No. of Pages	22. Price*
Unclassified	Unclassified	67	A04

*For sale by the National Technical Information Service, Springfield, Virginia 22161

NASA-Langley, 1982

National Aeronautics and Space Administration

Washington, D.C.
20546

Official Business
Penalty for Private Use, $300

THIRD-CLASS BULK RATE

Postage and Fees Paid
National Aeronautics and Space Administration
NASA-451

NASA

POSTMASTER: If Undeliverable (Section 158 Postal Manual) Do Not Return